A HYDROGEN ENGINE AND CONTROL CIRCUIT DESIGN

By

RICHARD GEORGE MURRAY

Bachelor of Science
Southern Methodist University
Dallas, Texas
1959

Master of Science
Missouri School of Mines
Rolla, Missouri
1962

Submitted to the Faculty of the
Graduate College of the
Oklahoma State University
in partial fulfillment of
the requirements for
the Degree of
DOCTOR OF PHILOSOPHY
May, 1970

A HYDROGEN ENGINE AND CONTROL CIRCUIT

DESIGN

Thesis Approved:

Roger K. Schroeppel
Thesis Adviser

J. A. Weibelt

Jack A. Allison

Allen M. Rowe

Dean of the Graduate College

PREFACE

This dissertation is concerned with contributing towards the development of a practical hydrogen burning engine, and more specifically with the development of an electrical circuit to synchronize the operation of a mechanical injection system where the fuel is hydrogen. This circuit, when assembled with a solenoid injector, speed, and demand power level input signal transducers will control the quantity of hydrogen fuel delivered directly into the cylinder of an internal combustion engine.

This dissertation is not concerned with the development of the solenoid injector or the input transducers. It proceeds with specifically assumed operating characteristics of these devices and outlines in the case of the solenoid injector, how changes in these characteristics can be compensated for in the electrical control circuit calibration.

I would like to express my sincere appreciation for the assistance and guidance given me by the following members of my Doctoral Advisory Committee: Dr. Roger J. Schoeppel, my Committee Chairman and Research Adviser, whose leadership and advice has made this project a success; Dr. John A. Wiebelt whose suggestions and directions were of great value; Dr. Allen M. Rowe for his enthusiasm and guidance;

and Dr. H. J. Allison for valuable suggestions in electronic system design.

In addition, I would like to thank the following individuals: Velda Davis for her typing and editing assistance; Mr. George Cooper for his technical assistance and extremely cooperative spirit; Mr. N. L. Freeman for his general assistance in the area of electrical technology; and Mr. Ray Ashcraft for excellence in component fabrication.

Finally, I wish to express appreciation to my wife, Nancy, and sons, Justin and George, whose encouragement, sacrifice, and patience were at all times a source of strength.

TABLE OF CONTENTS

Chapter Page

LIST OF TABLES

LIST OF ILLUSTRATIONS

CHAPTER I

INTRODUCTION

World's Present Energy Problem

American and world civilization is now faced with a sizable problem which affects the health and economy of nearly everyone and especially urban residents. This is the proper management of consumption and conservation of available energy resource and raw materials. Each day, today's industrialized society not only requires more energy and raw materials for each individual, but, also, numerous new individuals are brought into the sphere of this materialistic civilized world from the less developed societies.

Continuously increasing amounts of energy are being produced and consumed daily; essentially all of this energy comes from the combustion of fossil fuels, mainly, petroleum, natural gas, and coal. This fossil source is being increasingly used for raw chemicals, lubricants, plastics, and fertilizers. It is evident that today's civilization completely depends on an adequate supply of fossil fuels. It is also worth noting that fossil fuels burned today cannot be used for plastics and fertilizers tomorrow. Two undesirable side effects of large-scale fossil fuel combustion, both of which seriously threaten civilization, are:

contamination of the atmosphere with carbon monoxide, carbon dioxide, sulfur dioxide, and other combustion products; and depletion of the earth's atmospheric oxygen supply (1).

An Approach to a Solution

It seems obvious from the foregoing that it is desirable to limit the combustion of fossil fuels as much as possible. Wherever possible, the conversion of energy by combustion must be replaced through selection of a nondepleting, noncontaminating source such as nuclear, solar, or wind energy. Most electric power plants and ocean going vessels can be converted to atomic energy. Most domestic and commercial heating and power plants now operating on fossil fuels can be converted to electricity generated by this nuclear source. Rail and some other modes of transportation can likewise be converted to electricity.

There is, however, one major area of power generation that cannot conveniently or practically be converted to a noncontaminating form, by the above methods, and this involves the internal combustion engine. Vehicles and equipment using the internal combustion engine principle include: all land vehicles except an insignificant number which are powered by electricity; all aircraft, missiles and rockets; all portable power equipment not operated by electricity; occasional standby community power generation equipments. So far, no practical noncontaminating power generating device

has been devised that can replace the internal combustion engine in the private automobile.

Since some forms of the internal combustion engine are likely to persist for some time, it appears desirable to evolve the engine into a form that does not contribute to the contamination-depletion problem. The development of a hydrogen burning engine could be a practical answer to this problem.

If off-peak power from atomic, solar, or wind energy conversion plants were used to electrolyze water into hydrogen and oxygen and the oxygen were subsequently released to the atmosphere, not only would a high energy fuel be produced which would be nondepleting and noncontaminatory when burned, but also as much oxygen would be produced as would eventually be consumed when the fuel was burned. If then, the hydrogen could be used to fuel internal combusion engines, the exhaust products would not contribute (with the exception of oxides of nitrogen) to air contamination, oxygen, or fossil fuel depletion.

The need for an energy conversion device, such as a hydrogen burning engine is obvious. However, the development of such an engine depends on advancing technology in certain areas of combustion, engine design, and control. The remainder of this report will be a discussion of problems encountered in the development of a <u>research</u> hydrogen burning engine and the details of a prototype automatic control system developed to help make this engine a <u>practical</u>

reality. It is beyond the scope of this study to be concerned with the over-all aspects of production and storage of hydrogen, economic analysis, or the optimization of any given engine design.

It also should be emphasized that for a complete solution of air pollution and fossil fuel depletion, the proposed system is dependent upon the adoption of a total world energy package where prime energy resources are: nuclear, solar, hydrodynamic, and pneumodynamic.

CHAPTER II

LITERATURE SURVEY

Historical Review

Successful conversion of gasoline engines to burn hydrogen is reported as early as 1820 by Cecil (2).

Further practical development was demonstrated in 1932 by the German engineer, Erren (3), who designed and built several engines which could operate on hydrogen, conventional fuels, or mixtures of both. Engines as large as 100 hp were developed with compression ratios of up to 12 to 1. A thermal efficiency of 45% was claimed for one engine. Some models of Erren engines were equipped to operate on mixtures of hydrogen and gasoline or oil. One such engine, a 50 hp, 4 cylinder bus engine showed a 30% increase in power and 50% decrease in gasoline consumption when a small amount of hydrogen was added. An increased smoothness of operation was evidenced with added hydrogen which allowed the minimum idle speed to be reduced from 220 RPM to 159 RPM without misfiring or stalling.

A considerable amount of work was done immediately after World War II by King (4) and associates at the University of Toronto on the combustion characteristics of hydrogen as applied to internal combustion engines. In these

tests a Co-operative Fuel Research (CFR) engine was used to observe the combustion characteristics over a range of compression ratios from as low as 3.8 to 1 up to 10 to 1, and from very lean fuel-air ratios to very rich ones.

Recently, the National Aeronautics and Space Administration (NASA) sponsored two large research contracts aimed at development of an internal combustion engine using hydrogen and oxygen to produce electric power for spacecrafts.

One contract was with the Vickers Division, Sperry Rand Corporation, who developed a one-cylinder, liquid-cooled, side-head injector engine that produced over $4\frac{1}{2}$ hp at a minimum brake specific fuel consumption (BSFC) of 1.6 lb/hp-hr (5). This engine achieved a total of 619 hours of endurance testing with the longest continuous endurance run of 120 hours and with 5 runs of 65 hours each. In addition, 108 hours of performance testing were logged.

A second contract with the Marquardt Corporation, called for the conversion of an existing multi-fuel hypergolic engine to burn hydrogen and oxygen for possible use in the Lunar Excursion Module (LEM) (6). This engine was the same general type as the Vickers engine with the exception that it employed an overhead camshaft operated double-poppet valve injector system. Before completion of this phase of the project, the engine underwent a total of 3.2 hours of "hot" running with some runs of up to 43 minutes duration.

No other significant developments in reciprocating

hydrogen engine research are known to the author.

Properties of Hydrogen

With only few exceptions, hydrogen's characteristics as a motor fuel are quite comparable with common fuels such as gasoline (7). For instance, the minimum ignition temperature in air is 1065° F as compared to 1000° F for commercial butane; and the theoretical flame temperature in air is 3887° F as compared to 3615° F for butane. Distinctive characteristics of hydrogen are: its higher heating value of 53,500 BTU/lb as compared with approximately 20,000 BTU/lb for gasoline; its wide flammability limits in air of 4.00% to 74.2% by volume as compared with 1.9% to 8.6% for butane; its very fast maximum flame speed of 9.3 ft/sec in air as compared to 1.03 ft/sec for normal butane; and the fact that the hydrogen and oxygen occupy more volume before reaction than after.

Further Discussion of Chapter II

The high heating value of hydrogen indicates that it would be a desirable motor fuel; however, prior engine research has not been able to overcome the two principal problems: its high combustion temperature when reacted with pure oxygen, and its pronounced tendency to cause engine knock.

CHAPTER III

PROPOSED ENGINE SYSTEM

National Aeronautics and Space Administration research difficulties and engine component failures were primarily caused by the requirement to use pure oxygen as the oxidizer, which caused flame temperatures to increase to such a high value (from 3887° F to 5385° F) that even sophisticated engine components failed under prolonged exposure.

Research by Errin and King (2) (4) was plagued by a common difficulty: combustion problems such as detonation and preignition. This difficulty was brought about by the common attempt to carburet the hydrogen, or in other words to mix the hydrogen with the air before induction or compression. This attempt always resulted in either detonation or preignition. Even the CFR engine used in the Toronto research had to be stopped, dismantled, and thoroughly cleaned every 12 hours or engine knock would develop and interrupt the test.

Recognizing prior efforts, the project goal was set to perfect the hydrogen burning engine to a degree sufficient to supplement under certain conditions the fossil fueled engine.

Initial Design Concepts

For economy and reduced flame temperature, it was reasoned that the prototype engine should use air as the oxidizer. For simple and accurate speed control, it was decided that a throttle valve would be incorporated in the air intake system. Finally, it was decided to develop a hydrogen fuel injection system which will place the proper amount of hydrogen in the combustion chamber at or near the optimum time for combustion so as to promote smooth, detonation-free burning.

Procedure Used

Since the quantity of fuel to be injected and its appropriate ignition time are functions of engine speed, dilution of intake air by exhaust products, engine temperature, mass rate of flow of air, and manifold pressure, a two-step design procedure was selected to first demonstrate that reasonable compensation for these variables was possible, and second to build a second generation engine to more nearly optimize the interrelation of these variables.

The first phase was the construction of an engine incorporating a mechanical injection system which would serve as a research platform. This engine could possibly later be developed into the prototype of a practical mechanical injection hydrogen engine.

The second phase was to use performance data from the experimental mechanical injector engine to develop an

adjunct electrical injection system. This electrical injection system was to utilize manifold pressure and speed sensing devices to sense engine operationg conditions. These instruments would then relay a signal to a specially designed electronic control circuit which would determine when and how much fuel to inject for proper combustion at the demand power level. The injector control would, in turn, control a solenoid operated injection system containing double poppet valves with overlapped series operation for high frequency flow control for direct fuel injection into the combustion chamber. Volkswagon, at present, uses an electronic circuit solenoid valve system similar to that proposed herein. It controls the quantity of fuel delivered to the intake manifold as a function of engine speed, temperature, and manifold pressure; however, no attempt is made to inject directly into the combustion chamber or to accurately time when the fuel should be delivered to each cylinder (8). The fuel-air mixture is still inducted, compressed, and ignited in a conventional manner which would not be acceptable for a hydrogen system.

The success of the electrical injection engine design concept depended upon the development of acceptable mathematical relationships to predict engine fuel needs as a function of engine operating parameters, on the design of the control circuit to respond to these equations, and upon designing a solenoid operated injector that was capable of responding to the extremely short (approximately 15

milliseconds) time of each cycle. Preliminary design details for both the mechanical injection engine and the electrical injection engine will be presented in subsequent chapters.

The engine to be developed in phase one was to be equipped with adjustable injector linkages. Fuel flow measurements, engine operating temperatures, manifold pressure, and RPM would be taken for fixed operating conditions under various dynamometer loadings. This data would then be analyzed for the required mathematical equations to make the electrical conversion. The electronic control circuit would then be designed.

CHAPTER IV

ENGINE TEST APPARATUS PRELIMINARY DESIGN

Because of limited funds, the engine test apparatus was constructed, making maximum use of materials available in the Mechanical Engineering Laboratory and, in some instances, equipment loans from other departments.

Figure 1 shows a front view of the completed facility.

Dynamometer

A water brake dynamometer was mounted on a laboratory bench which became a platform for the entire test apparatus with its instrumentation. The compact arrangement also provided for easy transportation from area-to-area as needed.

Instrumentation

A steel reinforced three-fourth inch thick plywood panel attached to the front of the bench was used as both an explosion shield and an instrument panel. Two thicknesses of automotive safety sheet glass placed in a steel frame in the central section of the instrument panel provided for both safety and visual observation while the engine was operating.

The area of the instrument panel not taken up by the

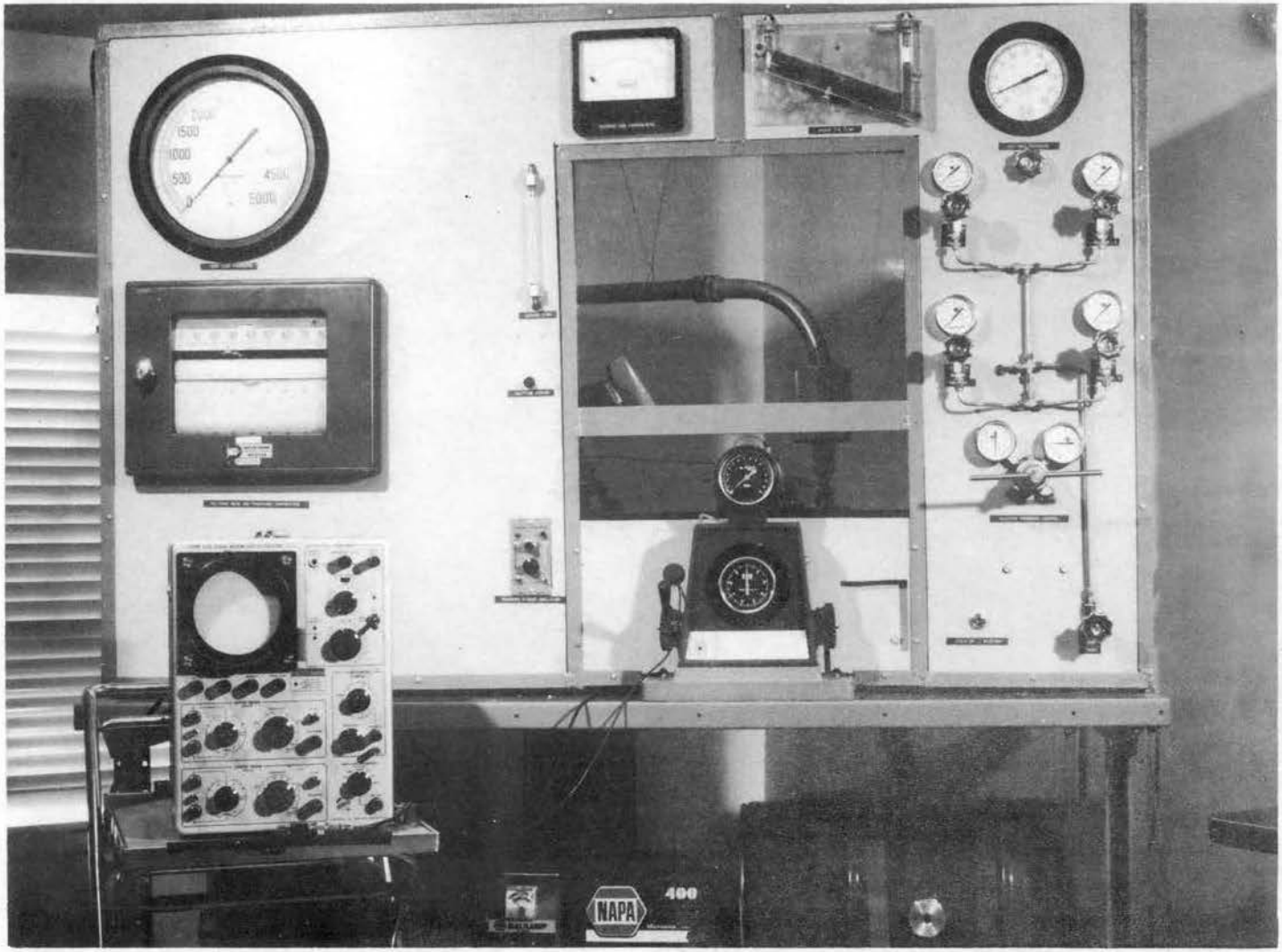

Figure 1. Engine Test Apparatus

window was divided roughly into two sub areas, one used for mounting engine operational control devices and the other for indicating and recording instrumentation. The operational control section contained among other things, a fuel delivery and control network designed for use with both the mechanical and electrical injection engines. The instrumentation section contains a multiple-point chart recorder for recording crankcase and cylinder head temperatures. Exhaust gas temperature is displayed on a separate meter above the observation window.

Flow of iso-octane fuel, used to determine a reference performance for the engine was observed by means of a floating ball rotameter. Engine intake air flow was determined by an ASME long radius nozzle, while hydrogen flow was determined by measuring pressure and temperature changes on a test tank of known volume over a known time.

Hydrogen Supply System

Gaseous hydrogen in high pressure bottles was used for the fuel source. These were attached to a common manifold and delivered hydrogen to a series of valves, pressure gauges, and a pressure regulator. A nitrogen purge system was included so that air could be purged from the system.

CHAPTER V

MECHANICAL INJECTOR DESIGN, DEVELOPMENT, AND OPERATION

The design scheme was to convert a standard production model engine to burn hydrogen as a fuel. This chapter is a discussion of the design, development, and operation of the prototype mechanical injection engine which resulted from an analysis of preliminary test results (see Appendix A) taken from the Briggs and Stratton 4 hp engine selected for conversion.

Injector

In order to prevent preignition, a direct combustion chamber injector was used. Since combustion starts very soon after injection and continues throughout injection, and since efficiency is dependent upon short combustion time, it is necessary to reduce injection time to as short an interval as practical. Assuming 50 degrees to be a reasonable injector gate angle (α) for an engine at a speed of $N = 4000$ RPM, there is only

$$T = \left(\frac{\alpha}{360}\right)\left(\frac{60}{N}\right) = \left(\frac{50}{360}\right)\left(\frac{60}{4000}\right) = 2.1 \text{ msec}$$

per injector cycle. This short time would lead to high

injector component stress, and difficulties in injector response to the drive mechanism if a single poppet were used.

Incorporating a dual poppet design similar to the valve used in the Marquardt engine (two concentric poppet valves using overlapped series operation to control flow) allows the inner valve to be opened as early as the beginning of the intake stroke, and the outer valve to be opened a few degrees before the beginning of the power stroke, the inner valve to be closed a few degrees after the beginning of the power stroke and the outer valve to be closed as late as the end of the exhaust stroke. This arrangement allows about

$$T = \left(\frac{\alpha}{360}\right)\left(\frac{60}{N}\right) = \left(\frac{360}{360}\right)\left(\frac{60}{4000}\right) = 15 \text{ msec}$$

per injector cycle which greatly decreases the required response of the injector mechanism. For this reason, it is clear that a dual poppet injector valve was a reasonable choice.

Injector Drive Mechanism

For simplicity in prototype engine design, the cam, cam follower, push rod, and rocker arm system shown in Figure 2 were chosen for initial testing. The camshaft had two lobes to operate the injector valve and was designed for variable injection duration and timing. A slotted collar arrangement on one cam lobe was the most practical approach to variable

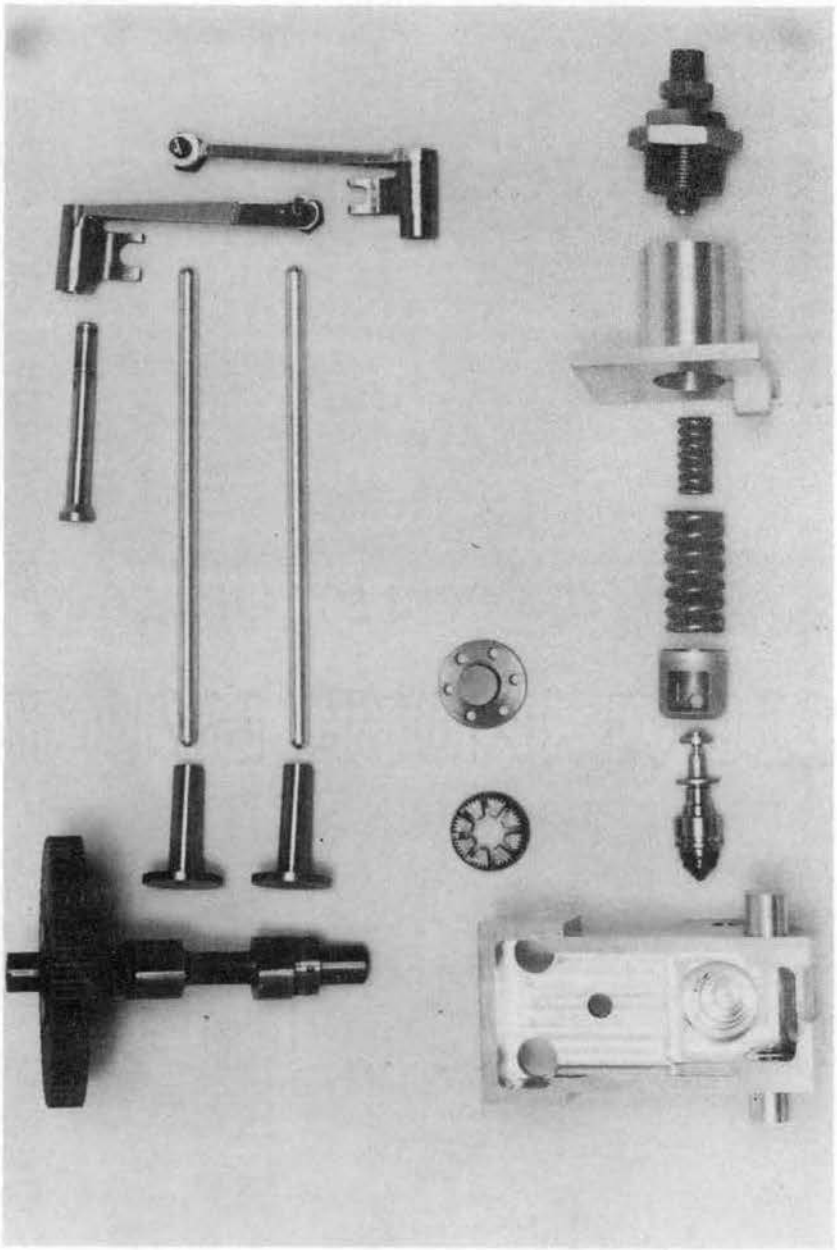

Figure 2. Injector Mechanism

timing in this case. This lobe when used as a replacement for the rear lobe of a standard B&S valve camshaft gear provided for variation in outer valve timing by stepping the camshaft gear on the crankshaft pinion, while inner valve timing and duration was achieved by stepping the rear lobe into various slots of the slotted collar.

Provision was made for installation of this second camshaft and its cam followers by weld insertion of an envelope into the side of the engine crankcase as shown in Figure 3. Pushrods transmitted the motion through rocker arms to the injector valve located in a housing fastened to the cylinder head. Figure 4 shows the completed engine assembly as it appeared during actual testing.

Timing

Crankshaft rotational degrees marked on a vibration dampening flywheel when used in conjunction with a pointer strobe-light arrangement provided visual reference to the engine's timing switch orientation. By relating this timing to a voltage step on an oscilloscope trace, the injector timing could be determined. This voltage step could be controlled by two switches in contact with the rocker arms, such that the voltage increased with the start of injection and fell with the end of injection.

Operation

On October 7, 1969, the Oklahoma State University

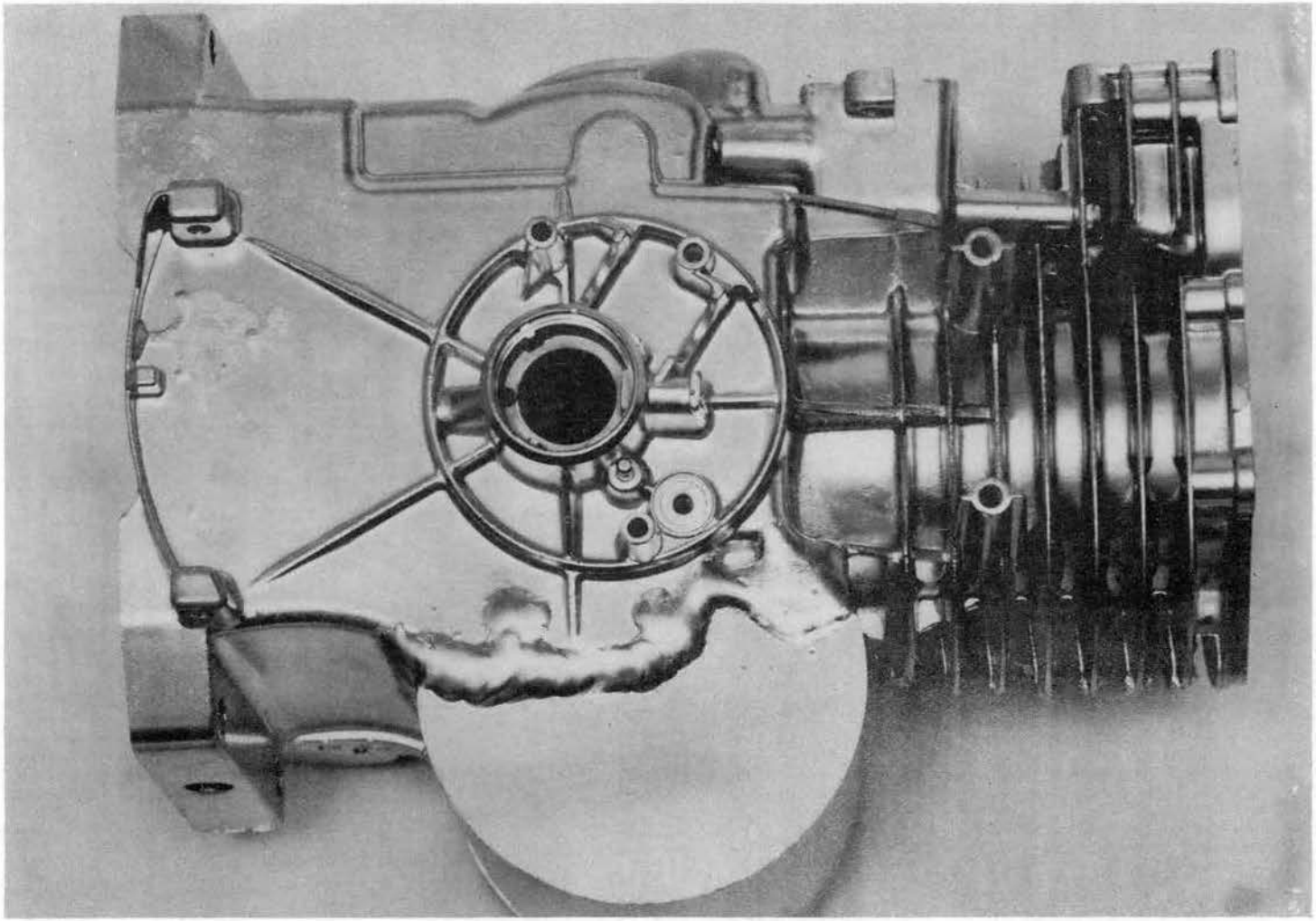

Figure 3. Crankcase

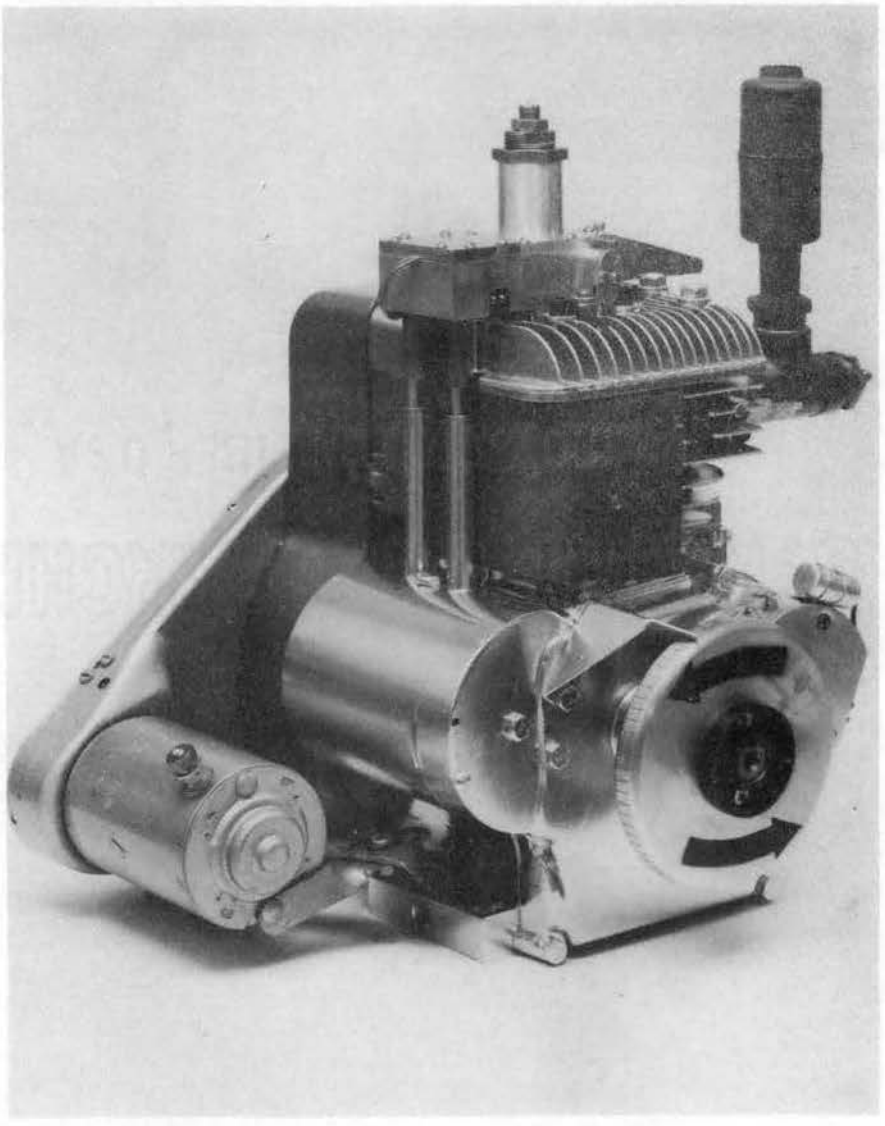

Figure 4. Hydrogen Engine Assembly

camshaft operated hydrogen fueled engine ran under its own power for the first time. Glow plug ignition was used and injection took place through a 0.060 inch orifice between 28° BTDC and 27° ATDC. Total running time for the first test period was 5.6 minutes.

Early in the hydrogen test phase, the decision was made to concentrate all experimental efforts on gaining operational experience and on a continuous modification process aimed at producing better performance. A second decision was that extensive engine performance testing could be postponed until such time as a near optimum engine had been developed.

The first modifications, relocation of the glow plug and an increase in the orifice diameter, yielded poorer engine performance. Subsequently, it was determined that an 0.018 inch diameter orifice used with an injector timing angle of 12° BTDC to 38° ATDC gave excellent combustion characteristics up to about 40% power.

Poor early engine performance while using glow plug ignition was apparently caused by low energy glow plugs and prompted adaptation of a conventional spark plug ignition system which proved an immediate success.

A redesign of the orifice plate and the installation of an internal combustion chamber duct for controlling the angle and area of hydrogen entry greatly reduced misfires and delayed combustion. This modification yielded knock-free combustion at significant power levels.

Test runs were then conducted over a range from 1200 RPM to 5000 RPM with prolonged power outputs of about 1 hp and momentary power demands of up to 2.25 hp. Results from two of these early hydrogen engine performance tests are presented in Table I.

A total running time of over 4½ hours with progressive improvement in combustion characteristics and general performance has been accumulated with this engine.

Summary of Chapter V

The above has described the development of a prototype model for procurement of experimental data needed in the design of the electrical injection engine. One additional outcome of this preliminary hydrogen experimentation was the experience gained in engine performance characteristics which set the direction for future design.

TABLE I

HYDROGEN ENGINE PERFORMANCE DATA

Property	Run 1	Run 2
RPM	3600	3500
Horsepower	0.75	0.98
Torque-ft. lb.	1.10	1.46
Fuel Air Ratio - lb. H_2/lb. air	0.73	0.66
Over-all Brake Efficiency-%	4	4
Specific Fuel Consumption-lb./hp-hr	1.27	1.24
Volumetric Efficiency-%	27	38
Brake Mean Effective Pressure-psi	15	21
Intake Air Temperature - °F	64	65
Exhaust Gas Temperature - °F	750	670
Cylinder Head Temperature - °F	540	490
Crankcase Temperature - °F	230	195
Manifold Pressure - in. Hg.	1.95	1.52
Spark Ignition Angle - degrees BTDC	12	12

CHAPTER VI

ELECTRICAL INJECTOR DESIGN ANALYSIS

Once sufficient data was acquired using the mechanical injector engine to predict engine operating characteristics, it was possible to design an electronic controlled solenoid operated injector mechanism to replace the camshaft drive system. This substitution provided more flexibility in adjusting injector response to engine fuel needs. To minimize the degree of redesign necessary in the prototype development, it was decided to retain the injector valve, rocker arm, and housing assembly of the mechanical injector engine.

Analysis of Iso-Octane Tests

Fundamentally, the fuel delivered to an engine acts basically as a heating agent for the air in the cylinder. Assuming proper combustion takes place, the engine will react in much the same manner regardless of the physical nature of the initial fuel. For this reason, the extensive data taken during iso-octane testing (see Appendix A for further details) can be used to predict the energy and fuel flow trends of the hydrogen engine.

Analysis of the iso-octane tests yields two important results: first, the behavior of maximum power fuel flow in relation to manifold vacuum and second, fuel flow as a function of engine RPM. Fuel flow versus manifold vacuum (see Figure 5) approaches a linearly decreasing function while fuel flow versus RPM (see Figure 6) was an increasing function.

Exhaust gas temperature at maximum power was found to increase nearly linearly with RPM, as shown in Figure 7, while cylinder head temperature remained nearly constant. If future research indicates the need, a maximum fuel injection limiting circuit could be built into the control unit to prevent excessive engine temperature.

Crankcase temperature remained relatively constant after warm-up for all normal operating conditions and could, therefore, be neglected as a parameter of mixture control.

Finally, it was reasoned from the iso-octane data, coupled with an appreciation for the rapid flame speed of hydrogen, that a linear increase in ignition angle with RPM would probably yield a satisfactory electric injector engine prototype.

Basic Circuit Functions

It became apparent from the preceding that two main electrical circuits would be needed to provide adequate mixture control over the entire range of normal engine operation: a timing circuit to start injection as a linear

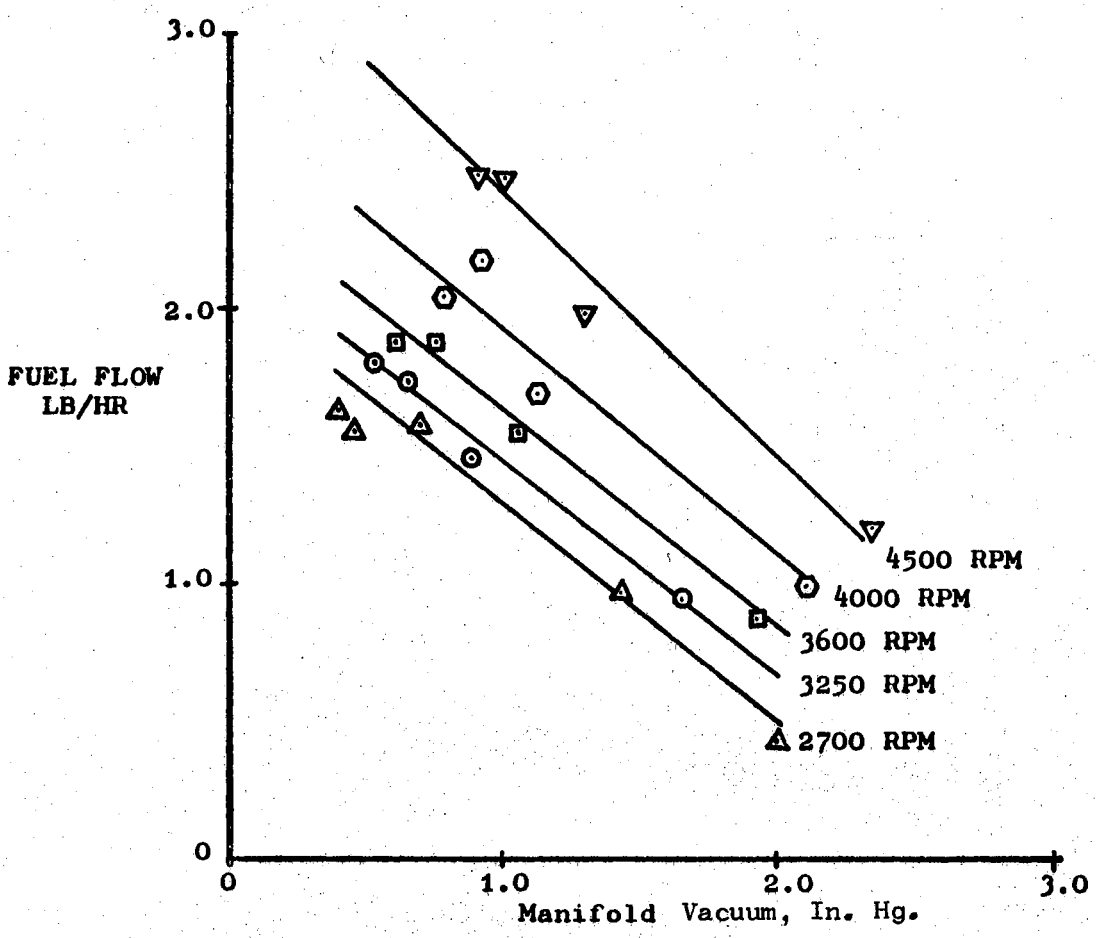

Figure 5. Fuel Flow vs Manifold Vacuum

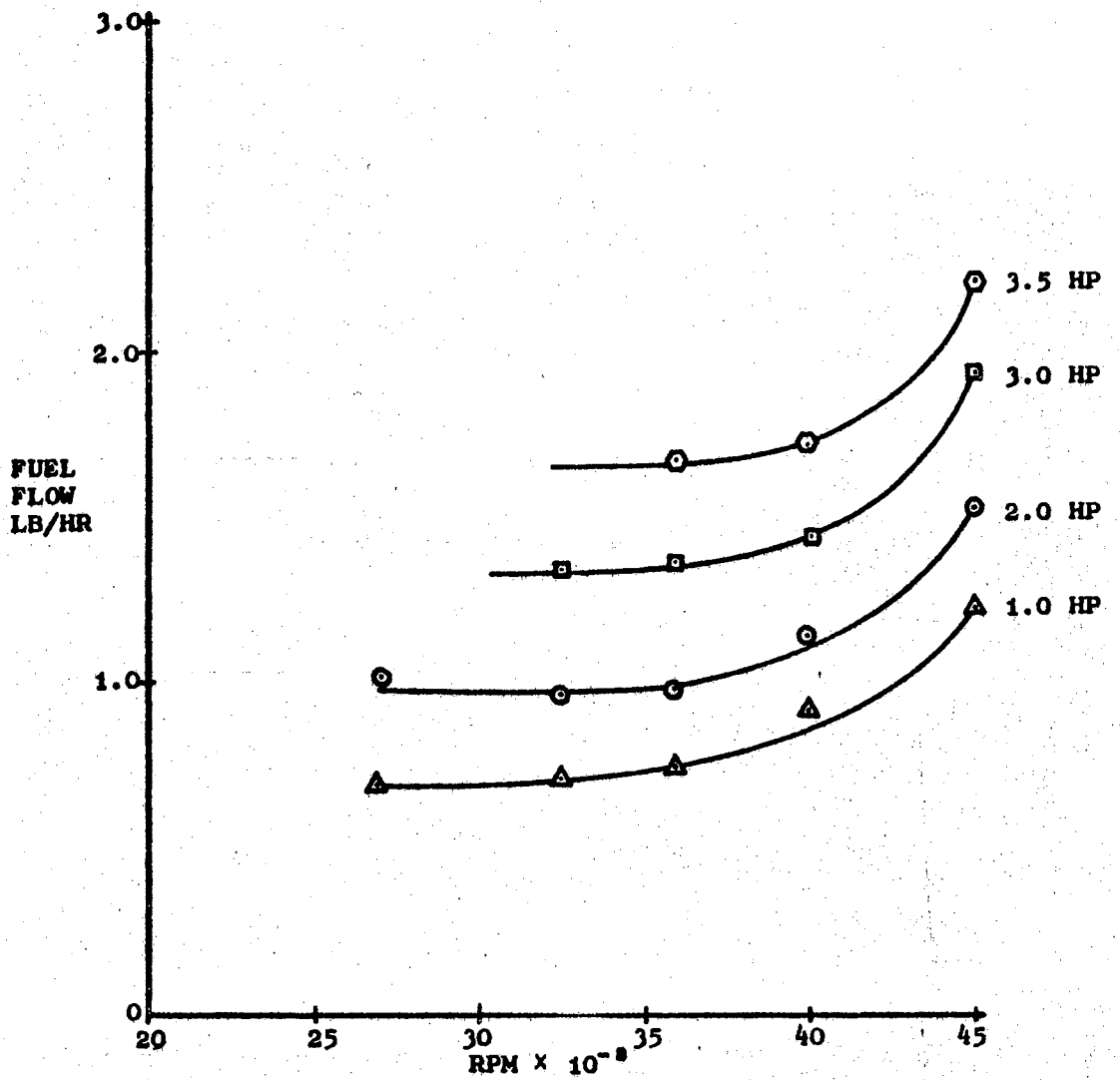

Figure 6. Fuel Flow vs RPM

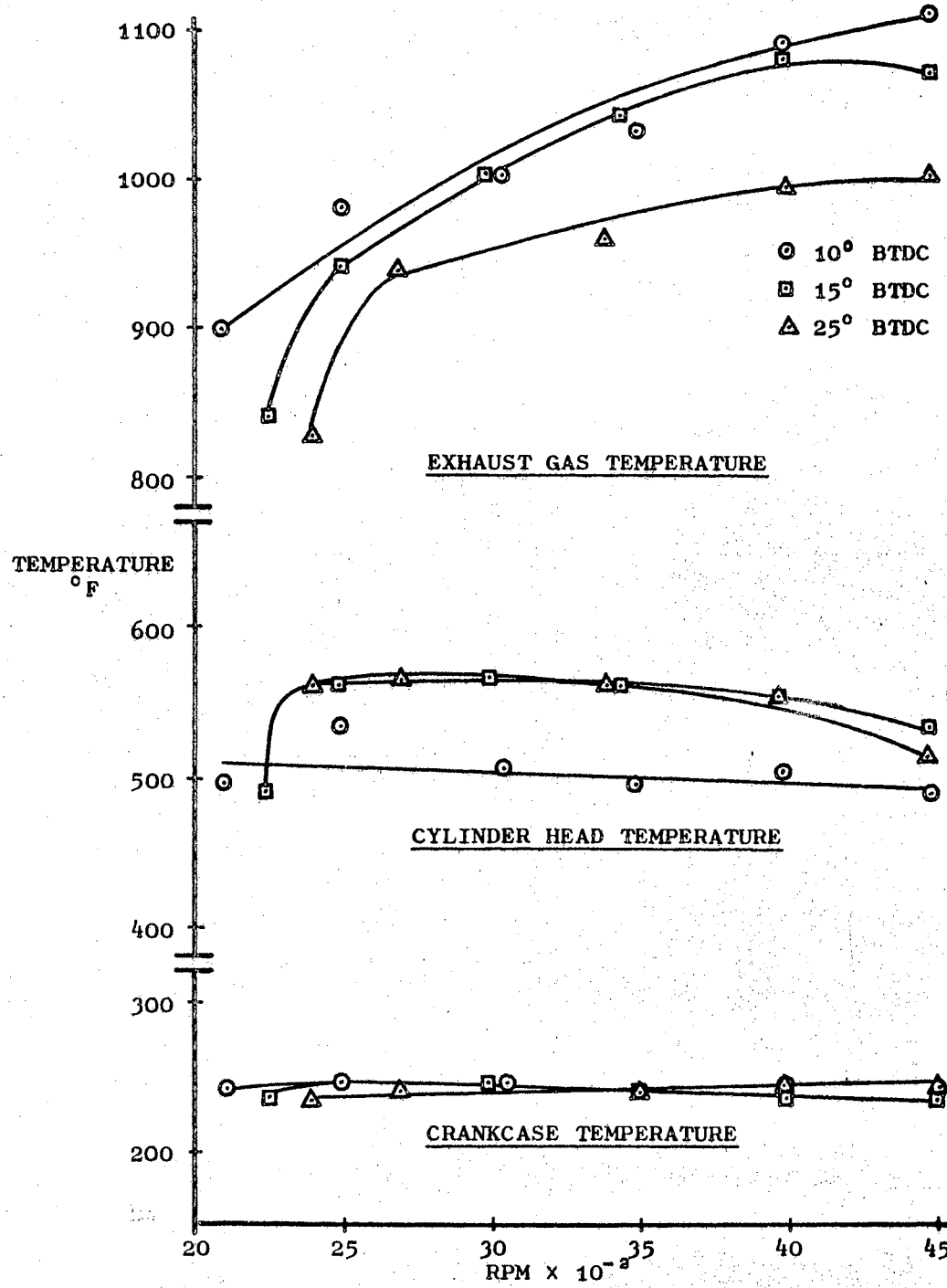

Figure 7. Engine Temperature vs RPM

function of RPM and a fuel flow duration circuit to deliver the proper quantity of fuel as a function of manifold vacuum and RPM. Figure 8 is a block diagram showing the basic layout of such a circuit. The two important input parameters, engine speed and loading, are relayed to the injector control circuit, which, in turn, delivers a power pulse of proper duration to the solenoid injector. Hereafter, the speed sensing device will be referred to as the RPM transducer.

Analysis of Injection Commencement Requirements

Engine Mechanical Behavior

The starting point of combustion in most engines is related to engine speed such that ignition timing is advanced in the engine cycle with an increase in RPM. This relationship is also desirable in the hydrogen engine since there will be a time delay involved in the transportation of the fuel from the injector to the combustion chamber and, as with other fuels, there is a finite time delay associated with the initiation of combustion.

A linear advance of the ignition angle with relation to engine speed has proved satisfactory for a large number of engine designs as related by Crouse (9). Taking into acacount the rapid flame speed of hydrogen, the linear advance curve of Figure 9 has been chosen as a suitable relationship. The equation for the chosen timing advance angle, θ_1,

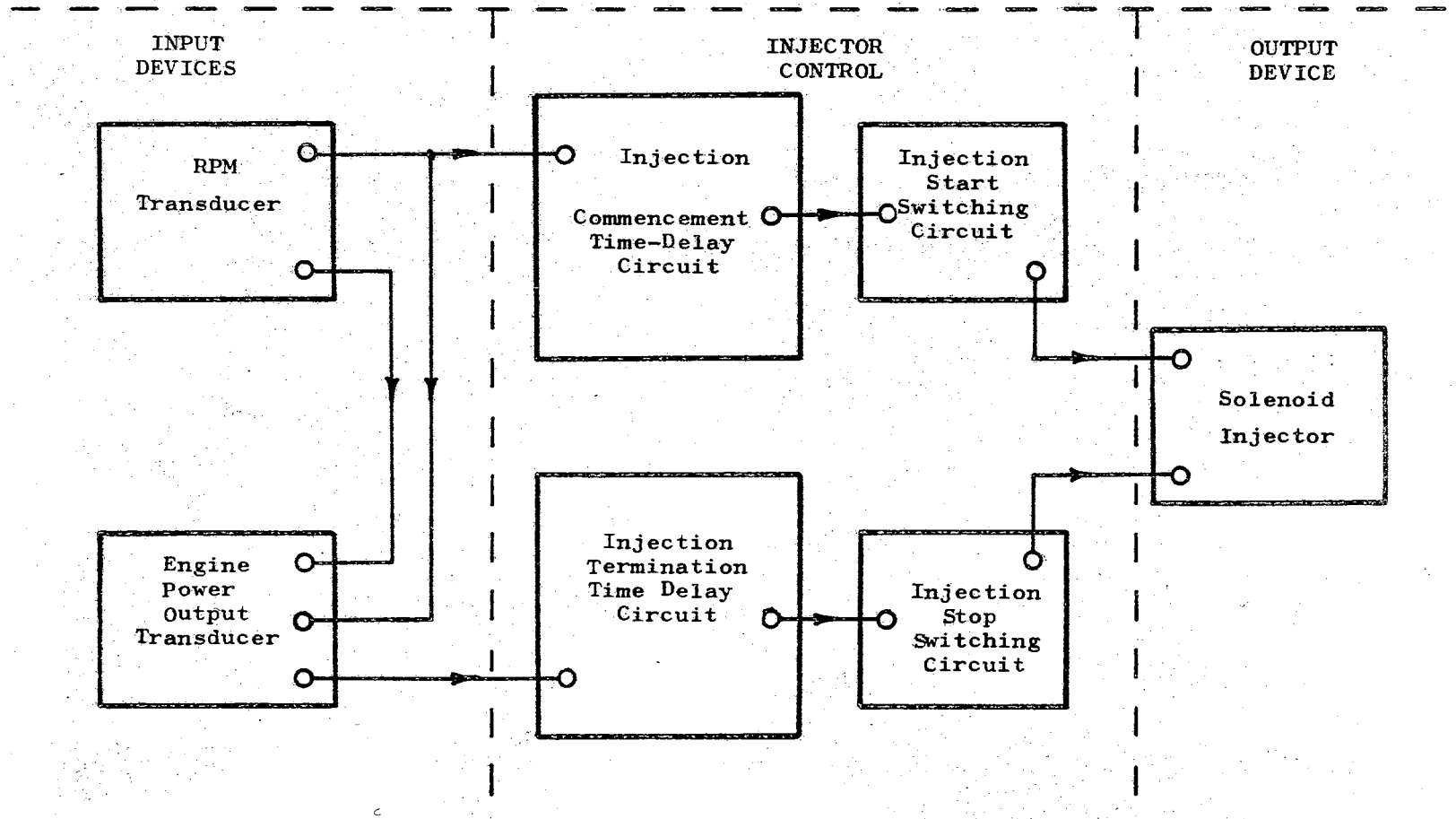

Figure 8. Complete Electric Injection System Block Diagram

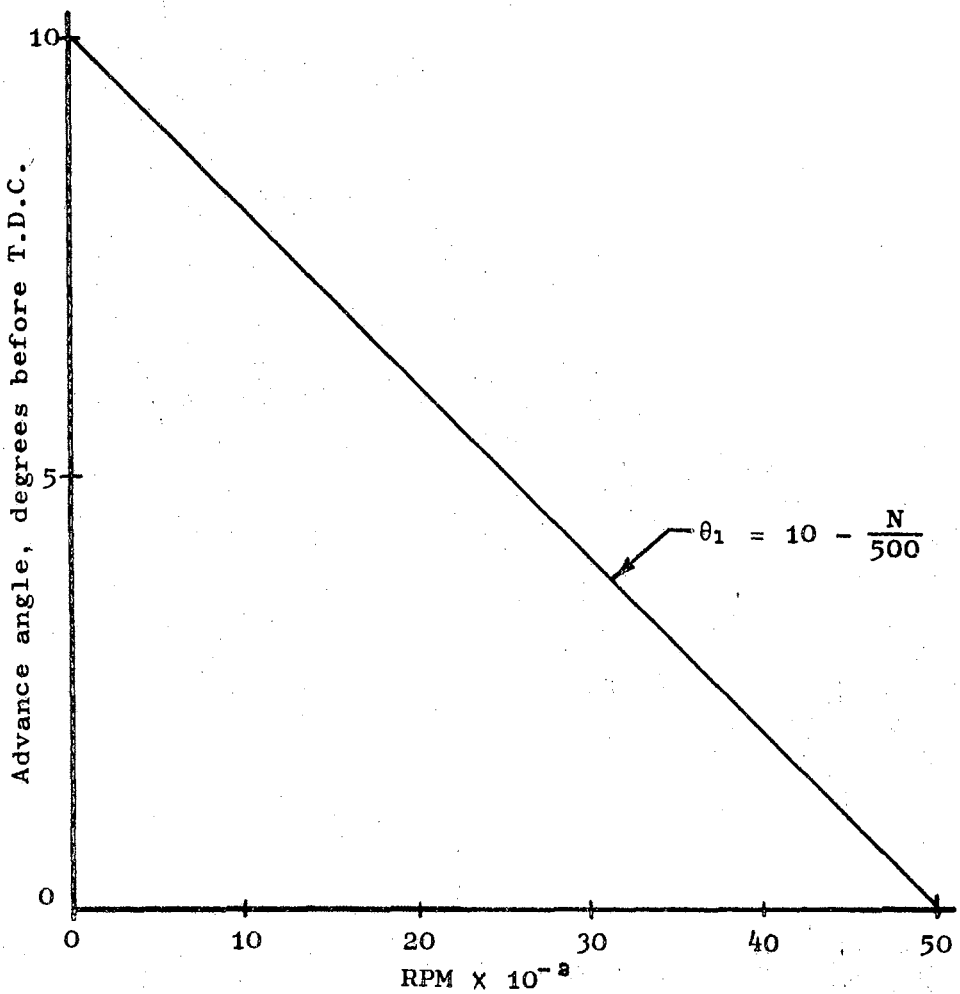

Figure 9. Injection Advance Angle

is

$$\theta_1 = 10 - \frac{N}{500} \text{ degrees}$$

where N is engine RPM.

The delay angle, θ_2, associated with a solenoid valve is

$$\theta_2 = 6Nt_s \text{ degrees}$$

where t_s represents the delay time between the initiation of the electric power signal and the activation of the injection valve plunger.

Assume for the moment that the electronic control cycle will be started by closing a camshaft driven switch at a predetermined angle, θ_T, and choose for the moment, an arbitrary minimum circuit delay time of one millisecond. At the maximum design speed of 5000 RPM, this delay time is equivalent to a delay angle, θ_3, of

$$\theta_3 = 6Nt = (6)(5000)(1 \times 10^{-3}) = 30 \text{ degrees.}$$

The timing switch preset angle, θ_T, can be set by summing the maximum condition of θ_1, and θ_2 at their maximum value, and by allowing the time delay angle of the circuit to be zero. Thus,

$$\begin{aligned} \theta_T &= \theta_{1max} + \theta_{2max} + \theta_3 \\ &= 10 + 6N_{max}\, t_s + 30 \\ &= 6N_{max} t_s + 40 \text{ degrees.} \end{aligned}$$

With the camshaft switch set at θ_T, the total angle under any operating condition can be represented by

$$\theta_T = \Delta\theta + \theta_2 + [10 - \theta_1] \text{ degrees}$$

where $\Delta\theta$ represents the required delay angle for the electronic circuit. Rearranging and solving for $\Delta\theta$ yields,

$$\Delta\theta = \theta_T - \theta_2 - 10 + \theta_1$$

$$= 6N_{max}t_s + 40 - N(6t_s + \frac{1}{500}) \text{ degrees.}$$

The corresponding delay time, t_d, associated with the mechanical action of the engine is

$$t_d = \frac{\Delta\theta}{6N}$$

$$= \left[N_{max}t_s + \frac{20}{3}\right]\frac{1}{N} - \left[t_s + \frac{1}{3000}\right] \text{ msec.} \qquad (1)$$

Taking a delay time, t_s of 5.1 milliseconds, which will be justified later, and the maximum design speed of 5000 RPM, this Equation (1) becomes

$$t_d = \frac{32.2}{N} - (5.4 \times 10^{-2}) \text{ msec.} \qquad (2)$$

Equation (2) represents the total physical time delay required between the closing of the camshaft switch and the supply of the electric power signal to the electric solenoid valve which starts injection.

Resistance-Capacitance Circuit Analysis

The graph of Equation (2) (see Figure 10) appears similar in shape to the general type of voltage curve one would expect from a resistance-capacitance (R-C) circuit. In such a circuit, as shown in Figure 11, the charge on the capacitor, q, is related to the capacitor voltage by

$$q = C\ E_c$$

where C is the capacitance. Current is the rate of change of charge, or

$$i = \frac{dq}{dt}.$$

Therefore, the voltage drop across the resistor is

$$E_R = iR = R\ \frac{dq}{dt}$$

where R is the resistance.

Writing Kirchoff's Law around the circuit

$$E_R + E_c = E$$

or

$$R\ \frac{dq}{dt} + \frac{q}{c} = E$$

and

$$\frac{dq}{dt} + \frac{q}{RC} = \frac{E}{R}$$

which is a first order differential equation that can be solved by separation of the variables to yield the

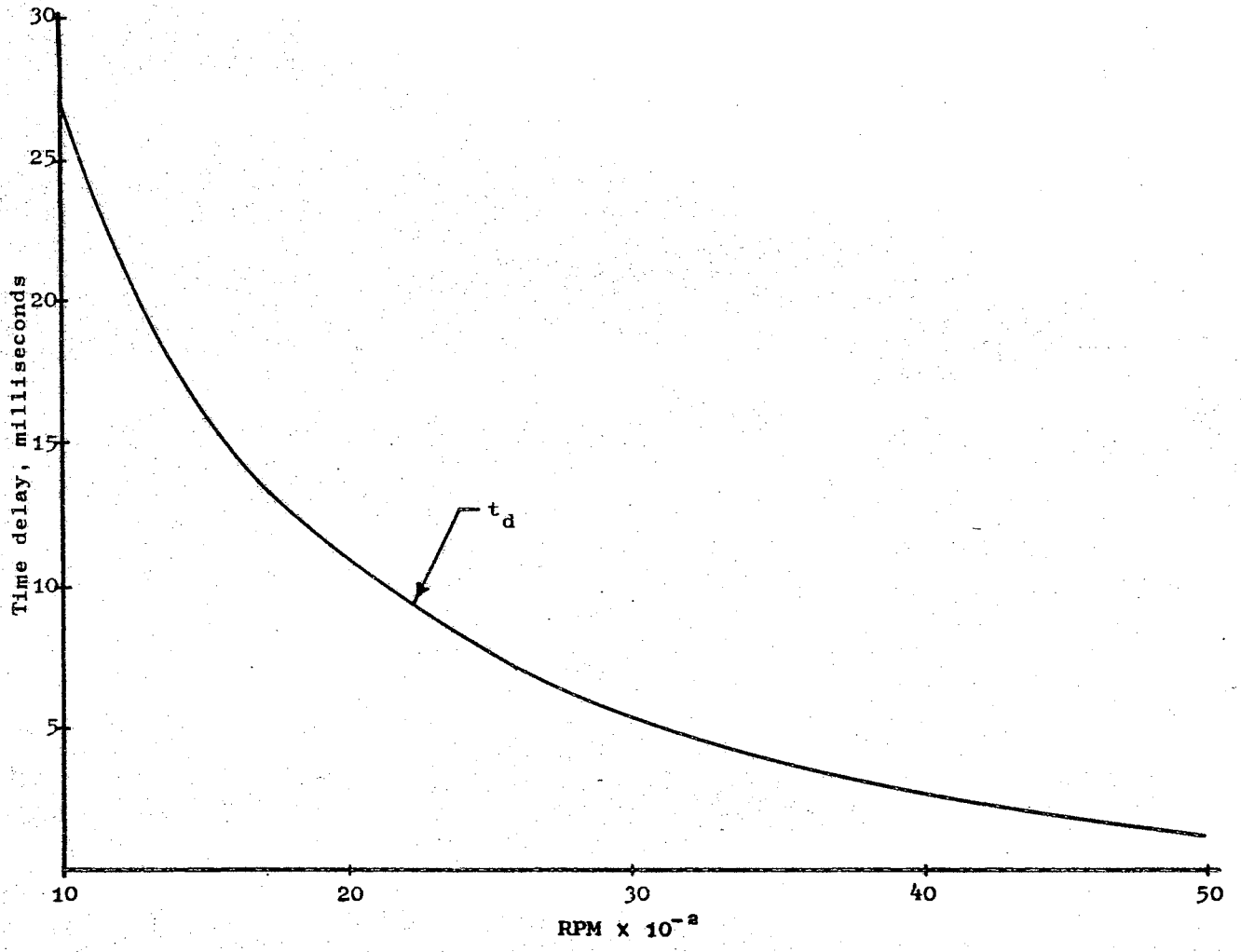

Figure 10. Engine Time Delay

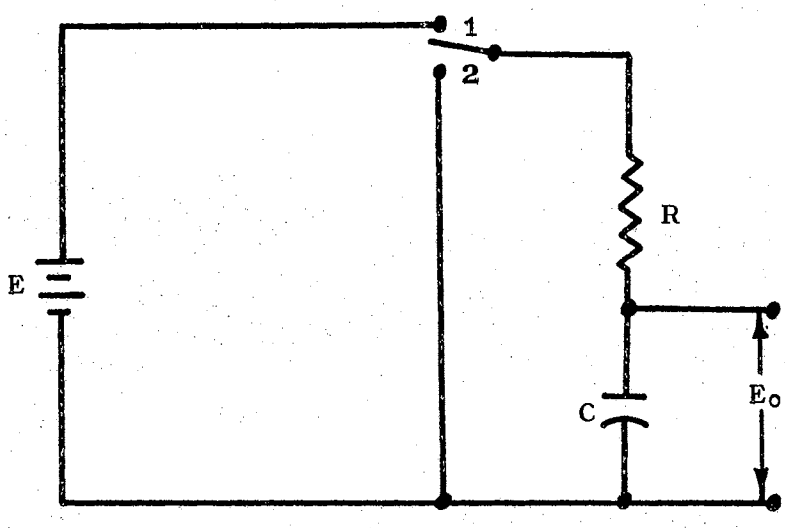

Figure 11. Resistance-Capacitance Circuit

complimentary solution

$$q_c = A \exp\left[-\frac{t}{RC}\right],$$

and the particular solution

$$q_p = EC,$$

and the complete solution

$$q = q_c + q_p = A \exp\left[-\frac{t}{RC}\right] + EC \qquad (3)$$

where A is a constant. Applying the boundary condition that at the instant the switch makes contact ($t = 0$) with terminal 1 (see Figure 11), the capacitor charge is zero ($q = 0$), Equation (3) becomes

$$q = EC\left[1 - \exp\left(-\frac{t}{RC}\right)\right].$$

The voltage across the capacitor is then

$$E_c = \frac{q}{C} = E\left[1 - \exp\left(-\frac{t}{RC}\right)\right].$$

Rearranging and solving for time yields

$$t = RC \ln\left[\frac{1}{1 - \frac{E_c}{E}}\right] \qquad (4)$$

which when plotted has a curvature of the same general shape as that of Equation (2).

Injection Commencement Timing Selection

With the aid of the computer program presented in Appendix B, which solves Equation (4) for various values of the voltage ratio, $\frac{E_c}{E}$, and various values of the multiplier, RC, a curve can be chosen such that its locus yields a solution of Equation (4) which closely approximates the engine requirements of Equation (2). The particular fit chosen in this case is shown in Figure 12 and has the parameters

$$RC = 0.0075$$

for

$$0.070 \leq \frac{E_c}{E} \leq 0.970.$$

The dashed curve on Figure 12 is a plot of Equation (2).

The maximum time error between the curves of Equations (2) and (4) (within the recommended operating range of this engine) is 1.5 milliseconds at 1500 RPM, which represents a timing angle error of 13 degrees before expected injection which is acceptable in normal engine design practice.

Injection Termination Analysis

Flow through the injection orifice is described by

$$\dot{m} = \rho AV$$

where $\dot{m}$ is the mass rate of flow, ρ is the fluid density, A is the orifice cross sectional area, and V is the velocity of the fluid. For a sonic condition at the throat of the

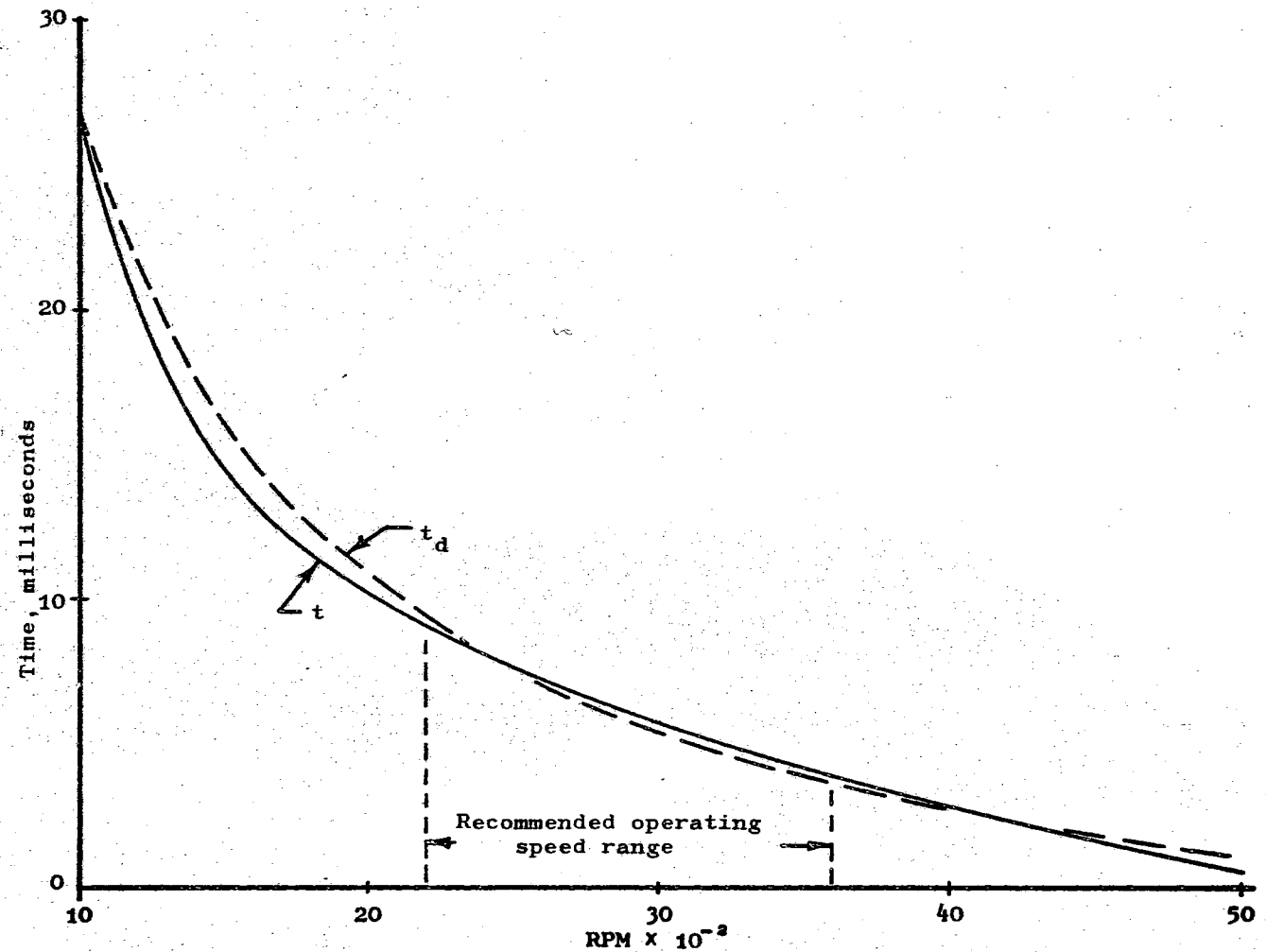

Figure 12. Injection Commencement Timing Curve

orifice, the velocity will be constant regardless of fluid downstream pressure. Then, for any given orifice area and a constant upstream pressure, which is a design consideration in this case, the mass rate of flow $\dot{m}$ will be a constant.

Under this condition, the mass of fuel delivered to the cylinder of the engine is dependent only upon the time of flow as shown by

$$M = \dot{m}t.$$

Therefore, the quantity of fuel delivered depends only upon injector valve open time.

Recalling from Figures 5 and 6, that fuel flow decreases with a decrease in RPM and power level (manifold vacuum), it can be seen that the choice of an injection termination curve, similar in shape to the electric circuit curve of Figure 12 but having a greater slope, can simulate engine injection time requirements.

By choosing a maximum injection angle after top dead center of 80° at 5000 RPM-maximum power and adding the 10° timing advance required at this RPM, the total injection angle equals 90° and the equivalent injection time becomes

$$t = \frac{\theta}{6N} = \frac{90}{(6)(5000)} = 3 \times 10^{-3} \text{ sec.}$$

Adding this to the injection commencement time curve at 5000 RPM, the maximum injection termination circuit delay time is 3.50 milliseconds. It is now possible to choose the maximum power injection termination curve extending between

the intersection of the injection commencement curve at 1000 RPM and the above injection termination point. This curve is represented by Equation (4) with

$$RC = 0.00750$$

for

$$0.365 \leq \frac{E_o}{E} \leq 0.970.$$

Figure 13 is a plot of injection commencement and termination time. By taking the difference between these two curves at various RPMs, a relative fuel flow (time) plot, such as Figure 14, can be constructed, which closely resembles the shape of the fuel requirements called for in Figure 7.

The dashed curve of Figure 13 represents injection termination at a reduced power level. The development of this curve will be explained in the power transducer section of Chapter VII.

Solenoid Switching

Silicon Controlled Rectifier Switching

The above analysis illustrates how the voltage rise across the capacitor of an R-C circuit can be used to simulate engine timing and fuel requirements. In order to complete the control circuit design, this voltage must be used to control the power to electric solenoids on the injector valve. In other words, a switching circuit must be designed

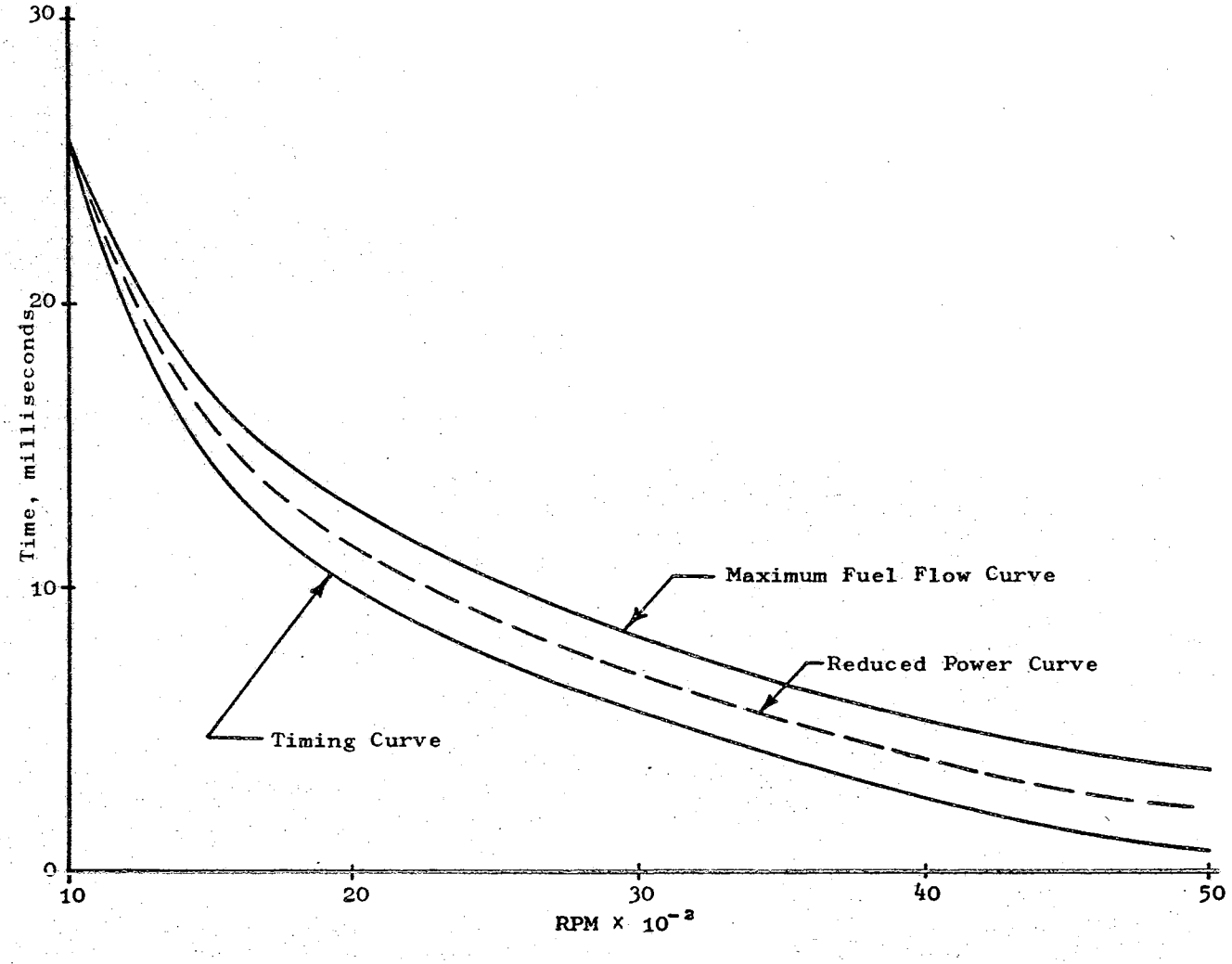

Figure 13. Injection Period Characteristics

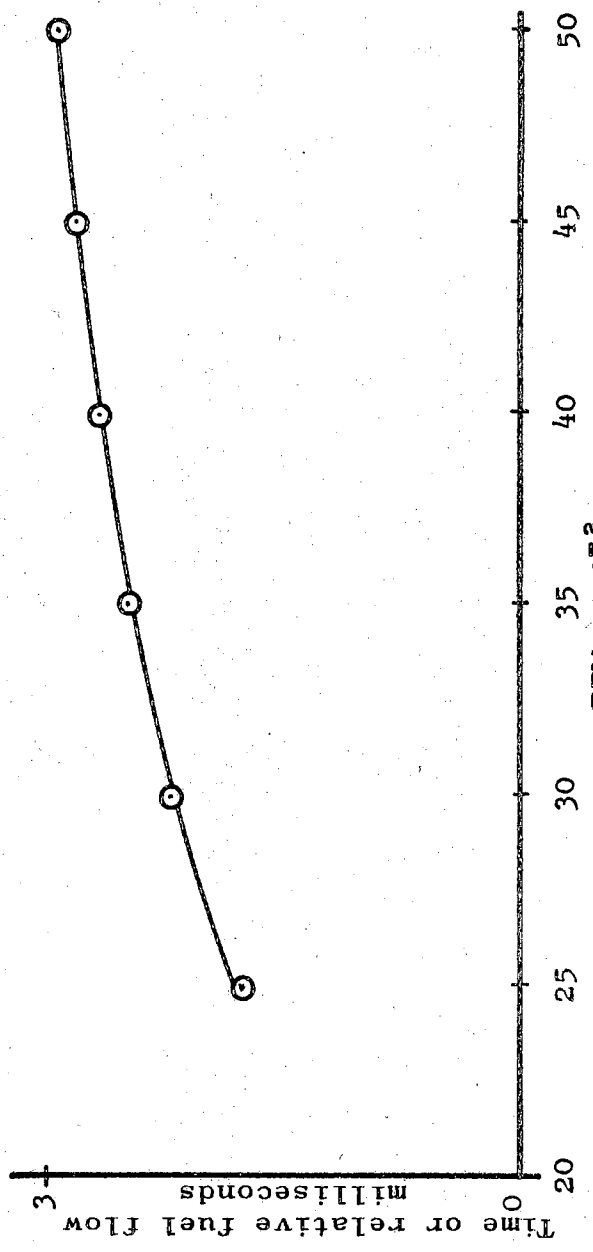

Figure 14. Relative Fuel Flow

that is sensitive to this voltage.

Basically, the silicon controlled rectifier (SCR) is a triode PNPN-type switch of the reverse blocking PNPN-type switch class (10). When sufficient current is applied to the gate terminal, the SCR switches to the "on" condition allowing the current in the power circuit to flow from the anode to the cathode. The SCR will remain in the "on" condition until such time as the power current drops to near zero even if the gate signal is removed.

In DC circuitry, the SCR turn-off situation is complicated by the fact that the DC voltage does not drop to zero or less as does AC voltage. Some auxiliary means must be used, therefore, to reset the SCR for its next switching cycle.

One such means is the flip-flop circuit which employs two SCRs, a resistor, the load device (in this case, a solenoid), and a capacitor as shown in Figure 15 (11). When a trigger signal is applied to the gate of SCR 1, it turns on, activating the solenoid and since the resistance of the resistor R is chosen higher than the resistance of the solenoid, the capacitor is charged to near line voltage through R. When a trigger signal is applied to the gate of SCR 2, it turns on, causing the capacitor to discharge, which, in turn, momentarily grounds the anode of SCR 1 causing it to turn off. The circuit is now reset and ready for its next switching cycle. One must be sure the gate currents are not applied to both SCRs at the same time or

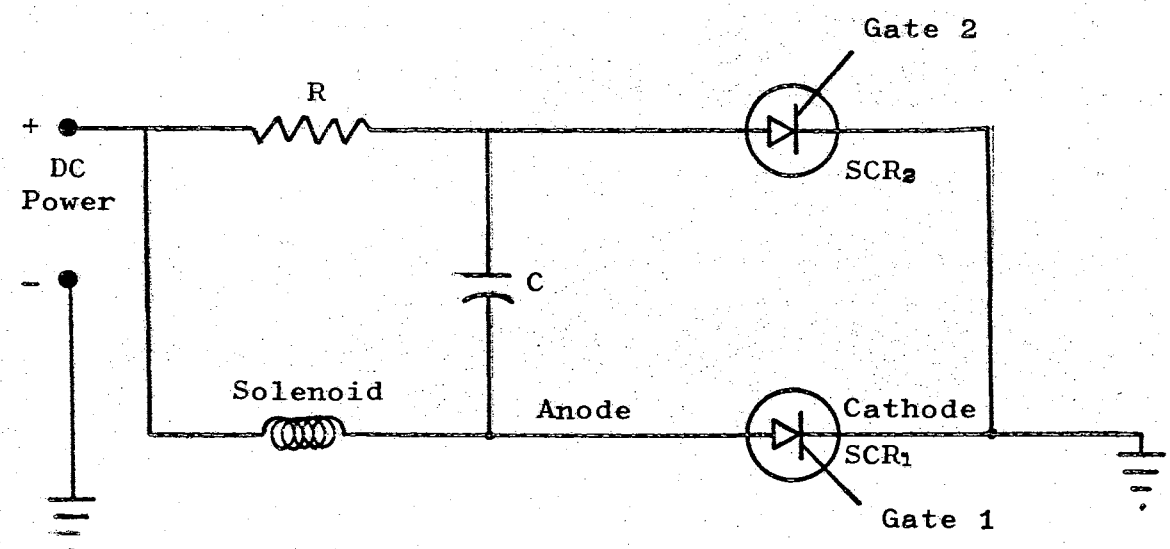

Figure 15. Flip-Flop Circuit

both will turn on and the circuit will become inoperative.

Unijunction Transistor Control

The basic difficulty with the SCR switching device is that it is turned on by gate current and not necessarily a definite gate voltage each cycle (11). To overcome this difficulty, a special type of unijunction transistor circuit may be employed as a triggering device for the SCR (12). As shown in Figure 16, this circuit consists of three resistors: R, R_1, R_2, a capacitor, and a unijunction transistor (UJT).

Operation of the UJT circuit requires that a voltage V_{BB} be supplied across the two bases of the transistor as well as R_1 and R_2. When a trigger signal voltage is applied to R and C, a voltage will build across C until it reaches the breakover voltage of the UJT at which time the emitter base 1 junction will go into the negative resistance region, discharging C through the UJT and the base resistor R_1. The discharge of C provides a pulse of sufficient current level to turn on the SCR. The breakover voltage is a function of V_{BB} and is a predictable and repeatable value.

It should be noted at this time that the R-C leg of the UJT circuit is equivalent to the R-C time delay circuit discussed previously for both the timing and fuel flow circuits.

Combined Control Circuit

By combining the injector timing circuit with the

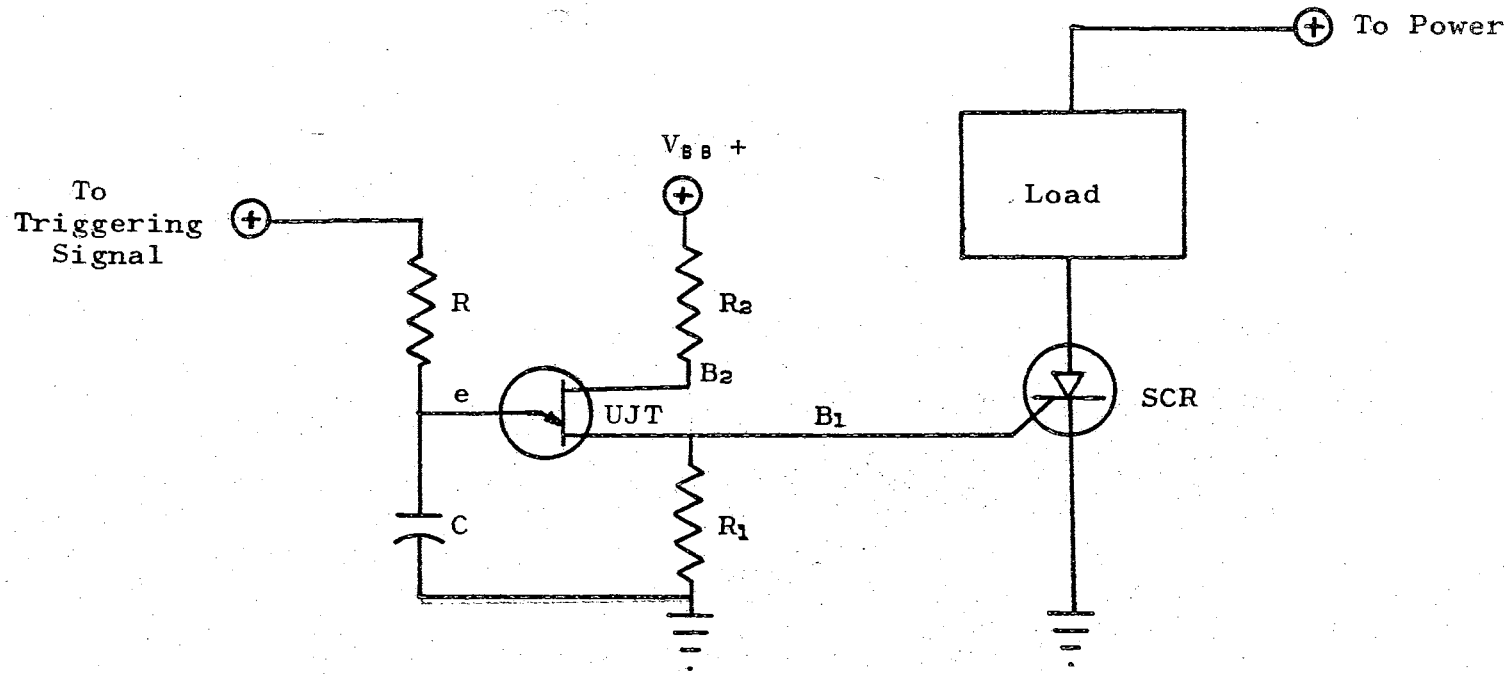

Note: e = emitter

B_1 = base one

B_2 = base two

Figure 16. Unijunction Transistor Timing Circuit

flip-flop switching circuit and by adding a camshaft reset switch, S_2, as shown in Figure 17, the control circuit package study is completed. A complete cycle description follows.

At the start of the injection cycle, the camshaft operated timing switch, S_1, makes contact, thereby placing the RPM transducer voltage on both the upper and lower UJT time delay circuits.

A time delay described by Equation (4) will occur before the voltage across the upper capacitor, C_U, builds up to the breakover voltage. Once this time has elapsed, UJT_1 will conduct, in turn, firing SCR_1, which will activate solenoid 1, L_1. Assuming solenoid 2, L_2, has previously been activated, fuel flow will now start. The RPM transducer voltage also acts on the lower UJT delay circuit through the power transducer which is a voltage divider. After the R_L-C_L circuit time delay has elapsed, the second transistor, UJT_2 will conduct, in turn, firing SCR_2 which momentarily grounds the anode of SCR_4 turning it off. This deactivates solenoid 2 and stops fuel flow.

The camshaft timing switch, S_1, is now opened and after a short delay, the camshaft reset switch, S_2, is closed. Capacitor C_3 discharges through resistors R_4 and R_5 resetting the upper and lower flip-flop circuits, thereby turning solenoid 1 off and solenoid 2 on. Capacitor C_3 also discharges through resistors R_6 and R_7 turning on SCR_5 and SCR_6 which allows capacitors C_U and C_L to discharge to

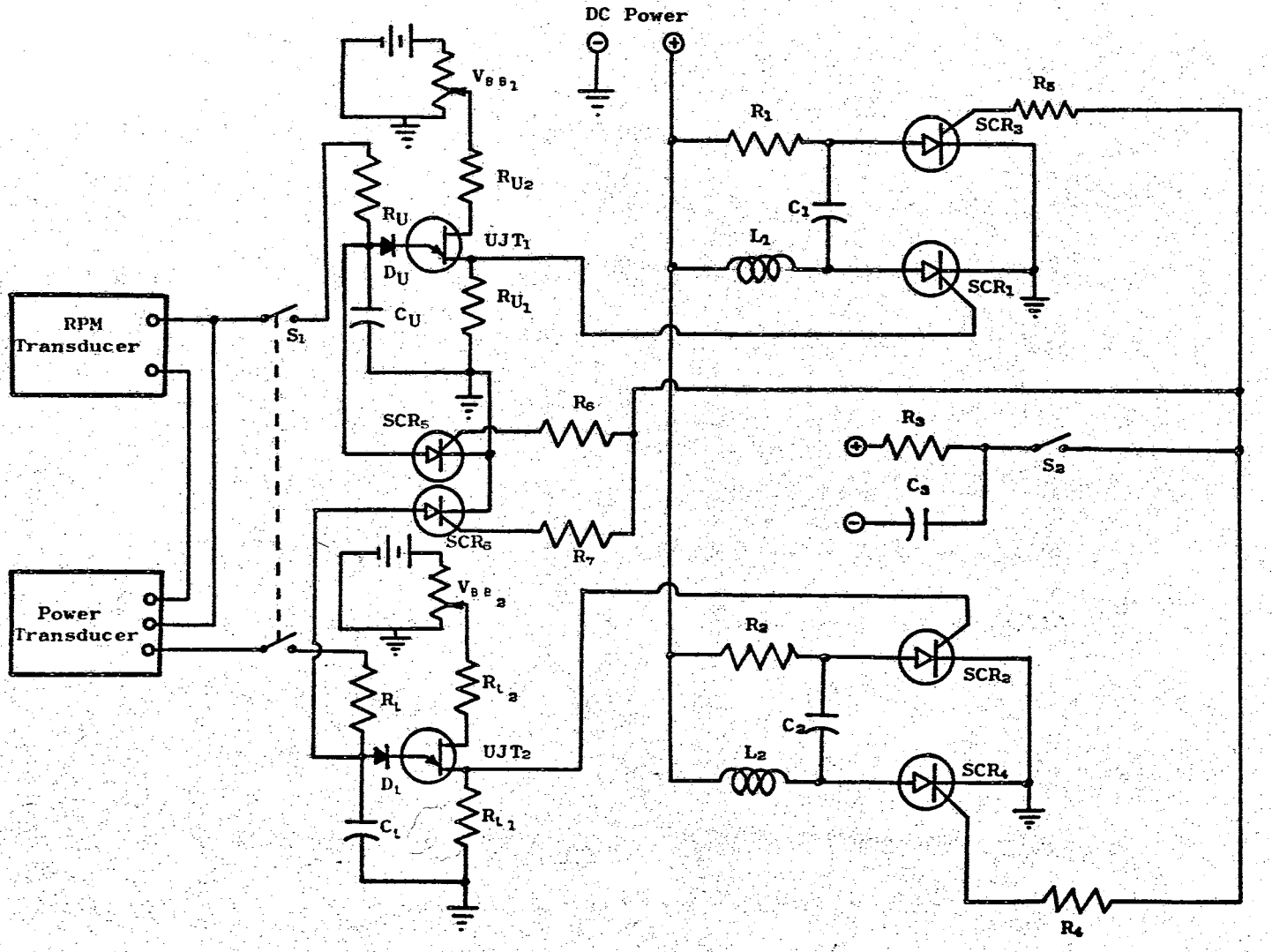

Figure 17. Complete Injector Control Circuit

ground. Once C_U and C_L have discharged, SCR_5 and SCR_6 automatically reset themselves to the "off" condition. Diodes D_U and D_L prevent any voltage build up on C_U and C_L due to leakage through the emitters from the bases. The camshaft reset switch now opens, recharging C_3 through R_3.

The two battery circuits associated with the UJT circuits are adjustable sources of DC voltages V_{BB_1} and V_{BB_2} supplied to the bases of the transistor circuit.

Summary of Design Analysis

From the above analysis, it is evident that the proper employment of the two R-C time delay circuits with two flip-flop switching circuits provides a response which closely resembles the timing and fuel flow needs of the design engine.

It should be remembered that the foregoing design is dependent upon the assumption (which was also justified) that the general fuel trends for this engine operating on hydrogen will be similar to its operation on iso-octane. Also, it should be emphasized that for these design conditions, fuel flow will automatically be cut off below 1000 RPM.

CHAPTER VII

DESIGN AND FABRICATION OF THE CONTROL CIRCUIT

Separate design teams have been assigned the job of developing the three accessory items associated with this control circuit: the RPM transducer, the power transducer, and an improved solenoid injector valve.

The author has undertaken the task of showing that the circuit described in Chapter VI can be developed into a reality and does, in fact, perform in a manner that yields satisfactory engine performance when combined with the engine transducers and injector valve.

Solenoid

In order that a representative solenoid pick-up time, t_d, be used in Equation (2) and to observe actual-dynamic injector valve operation, it was necessary to test a preliminary solenoid before starting circuit design. It should be emphasized at this point that if a different solenoid injector valve should be selected, its pick up time very likely will be different, and, therefore, will require a separate solution of Equation (2). The basic design procedure to be outlined hereafter will remain the same, however, regardless

of solenoid pick-up time.

It should also be noted that a different solenoid should be used in future research for the following reasons: first, an improved design could eliminate the heavy, rocker arm, and plunger masses associated with the present conversion of the mechanical injector mechanism, thereby eliminating harmonic resonance and friction. Second, shorter pick-up times will allow a corresponding decrease in the camshaft switch preset angle, θ_T.

In order to make most efficient use of available time and for reasons of economy, a commercially available 24 volt DC intermittent duty 10 pound pull, 15 ohm, solenoid was selected. It was found that the pick-up time of this solenoid was approximately 13 milliseconds which was too slow to allow activation, deactivation, and a reasonable dwell period under high RPM conditions.

To stimulate the pick-up time, an overvoltage system was incorporated such that 44 volts DC was supplied to a 15 ohm resistor placed in series with the solenoid. By applying this increased voltage at the time the switch was closed, the instantaneous rate of change of current, di/dt, was quite high, which, in turn, produced an increase in solenoid force. As more current began to flow in the circuit, an increasing IR voltage drop occurred across the resistor until at steady state, 22 volts were applied to both the solenoid and the resistor. This procedure reduced the solenoid pick-up time to a satisfactory 5.1 milliseconds

and yet kept the current flow to a low enough level that solenoid overloading was prevented.

SCR Switching Circuit

The two flip-flop circuits of Figure 17 are identical and were assembled on an aluminum chassis so that heat generated within the SCRs could be dissipated. SCRs of the 3 amp 2N3228 type were chosen in all four cases. The resistance R_1 and capacitance C_1 were chosen at 1000 ohms and 1.0 microfarad, respectively. This allowed a current flow through the resistor of only

$$I = \frac{E}{R} = \frac{44}{1000} = 44 \text{ milliamps},$$

a sufficiently small recharge time constant of

$$R_1 C_1 = (1000)(1.0 \times 10^{-6}) = 1 \text{ millisecond},$$

and yet enough charge in the capacitor to reliably turn off the power SCR.

Reset Circuit

The reset circuit must contain enough energy to reset SCR_3, SCR_4, SCR_5, and SCR_6, of Figure 17, and yet have a sufficiently short time constant to allow the capacitor to charge at high RPM. It was determined that a capacitance, C_3, of 2.0 microfarad and a resistance, R_3, of 1000 ohms gave adequate energy with a sufficiently short 2 millisecond time constant. Resistances R_4, R_5, R_6, and R_7 were all set

at 27 ohms which was high enough to prevent the entire reset current from going into any one conducting SCR gate leaving the others without reset energy, and yet large enough to prevent an excessively high gate current. Type 2N3228 SCRs and type 1N2071 diodes were chosen for the reset circuit primarily because of their availability.

Unijunction Transistor Time Delay Circuit

Base Circuit

The base circuits of both the upper and lower UJT circuits of Figure 17 are identical. The base two resistance was selected at 100 ohms which is consistent with normal design practice as related in the Silicon Controlled Rectifier Manual (11). In a similar manner, the base one resistance was set at 27 ohms.

Unijunction transistors of the 2N2646 type were selected in both circuits primarily for their low price. General characteristics of this device are given in the General Electric Transistor Manual (13).

Emitter Capacitor

Two factors controlled the selection of the two emitter capacitors C_U and C_L. The first was the requirement that the capacitor have a sufficiently high capacitance to maintain the voltage at the UJT base one after triggering, so that an adequate current pulse was available to the gate of its associated SCR.

The second requirement was that the $R_U C_U$ and $R_L C_L$ time constants must match their respective characteristic curves as previously described in Figure 13.

For both the upper and lower circuits, a capacitance of 0.2 microfarad and a resistance of 37.5K ohm satisfied the energy needs of the SCR and produced a multiplying factor for Equation (4) of

$$RC = 0.0075.$$

Theoretical RPM Transducer Input Requirements

As previously stated, when the voltage across the emitter capacitor of a UJT circuit reaches the breakover value, the UJT conducts and the associated SCR is triggered. This breakover voltage then becomes the capacitor voltage E_c in Equation (4). Furthermore, the voltage applied to the resistor of the R-C emitter circuit combination becomes the voltage E in Equation (4).

The ratio E_c/E is the curve shaping term that matches the electric circuit time of Equation (4) to the engine mechanical time of Equation (2). The dependent variable, E, in this ratio, therefore, becomes the factor that forces the time delay and switching circuits to respond to engine needs. E_c can be adjusted over a reasonable range by changing the base voltage V_{BB} (Figure 17). However, once E_c has been selected by the calibration of V_{BB}, it is a set value. The allowable range of E_c/E for both the timing and fuel flow delay circuits were given in Chapter VI.

Accordingly, the theoretical RPM transducer voltage outputs is defined for any selected E_c.

For the timing circuit, the value of V_{BB} was selected at 5.97 volts which for the particular UJT yielded a break-over voltage of E_c of 4.87 volts. Relating this value of E_c to the output of the computer program in Appendix B, Table II was tabulated which, in turn, allowed the theoretical timing circuit-RPM transducer curve of Figure 18 to be drawn. In this figure, E_t is the timing circuit voltage, while E_p is the fuel flow circuit voltage. Similarly, for the fuel flow circuit, with V_{BB} equal to 6.16 volts, E_c takes on the value of 4.87 volts. Relating this value to the output of the program of Appendix B, allowed Table III to be tabulated and the theoretical power circuit-RPM transducer curve of Figure 18 to be drawn.

Power Transducer

The criteria for determining the required power transducer function follows from an examination of Figures 6 and 13. Equation (4) is the function generating the upper curve of Figure 13. This curve represents fuel flow termination time for a maximum power condition. For any lower power level, it becomes necessary to terminate fuel flow at an appropriately earlier time.

An examination of the various power curves of Figure 6 shows that at a constant RPM within the normal operating range of the engine, a multiplying factor of approximately

TABLE II

TIMING CIRCUIT THEORETICAL INPUT VOLTAGE

RPM	$\frac{E_c}{E_t}$	E_t
5000	0.0650	74.92
4500	0.1750	27.83
4000	0.2900	16.79
3500	0.4000	12.18
3000	0.5150	9.46
2500	0.6300	7.73
2000	0.7450	6.54
1500	0.8550	5.70
1000	0.9700	5.02

TABLE III

FUEL FLOW CIRCUIT THEORETICAL
INPUT VOLTAGE

RPM	$\frac{E_c}{E_p}$	E_p
5000	0.3700	13.16
4500	0.4450	10.94
4000	0.5200	9.37
3500	0.5950	8.18
3000	0.6700	7.27
2500	0.7450	6.54
2000	0.8200	5.94
1500	0.8950	5.44
1000	0.9700	5.02

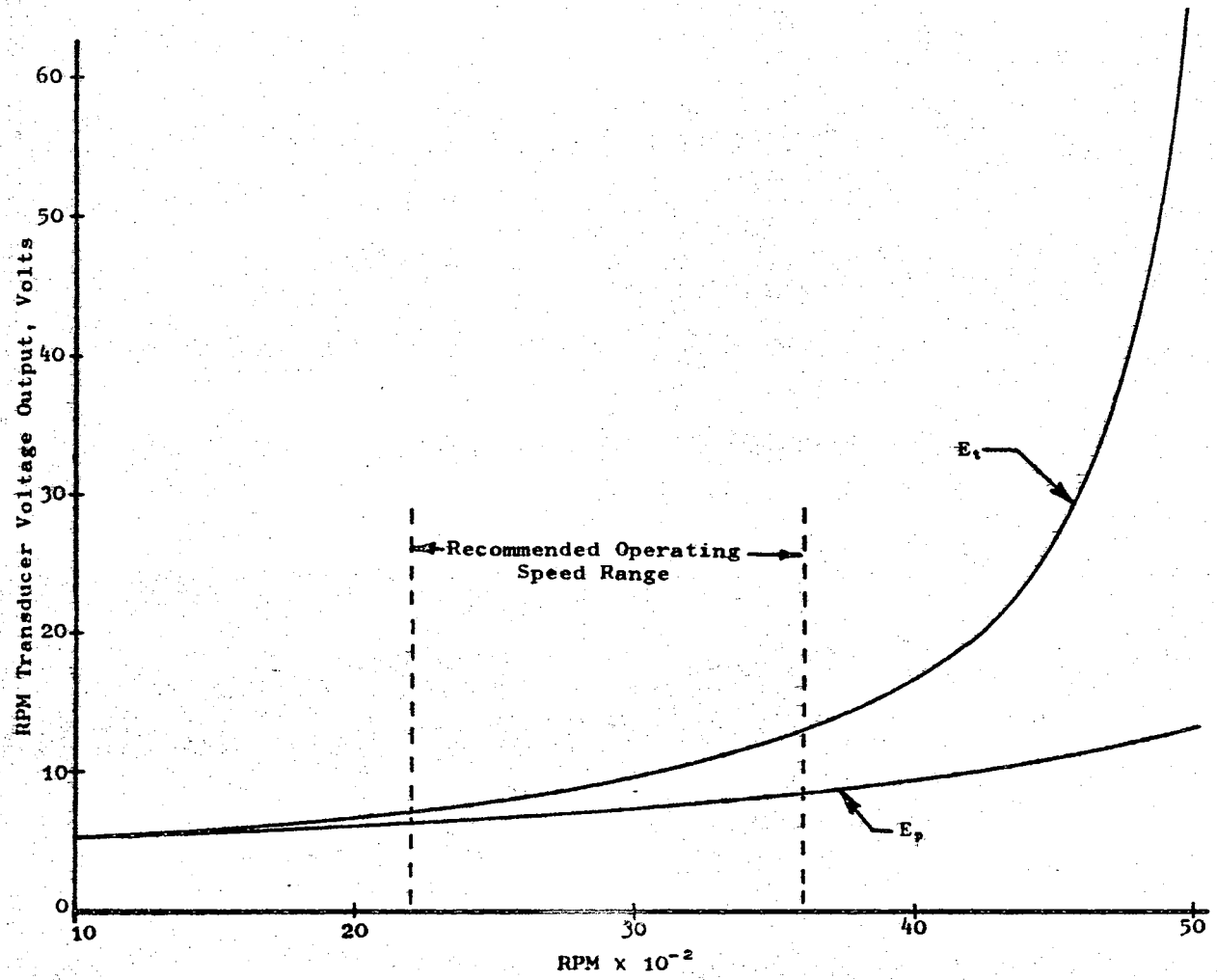

Figure 18. RPM Transducer Voltages

1.25 on the fuel flow time (and correspondingly on injector open time) yields the next higher horsepower curve.

On a percentage basis, using 3600 RPM as a basis, the decrease in fuel flow between three horsepower and two horsepower is

$$100\left(\frac{1.35 - 1.00}{1.35}\right) = 25.9\%.$$

In a similar manner between two horsepower and one horsepower, the decrease is

$$100\left(\frac{1.00 - 0.75}{1.00}\right) = 25.0\%.$$

Or, in other words, approximately a 25.4% decrease in fuel flow or flow time is required for each unit reduction in horsepower.

Figure 5 shows a generally linear decreasing slope of 1.2 inches of mercury per horsepower, therefore, by combining the information from both curves, one can determine the fuel flow time percentage as a function of manifold vacuum to be

$$\frac{25.4}{1.2} = 21.5\%$$

or a 21.5% decrease in fuel flow time for each inch of mercury increase in manifold vacuum.

By using the voltage divider technique between the voltage output of the timing circuit function generator, E_t, and the voltage output of the maximum power function

generator, E_p, any proportion of these two voltages can be delivered to the power time delay circuit (see Figure 19). Appropriately, under full power conditions, this circuit would receive a voltage, E_p, and at no-load conditions it would receive a voltage very close to E_t.

Preliminary design analysis of the power transducer indicates that it could be a manifold vacuum sensitive mechanism such as a spring loaded diaphragm which drives the above voltage divider (a 500Ω potentiometer) through a suitable linkage such that, for each inch of mercury increase in manifold vacuum, the time delay of the fuel flow circuit will be 21.5% shorter.

As mentioned earlier, the dashed curve of Figure 13 represents a plot of fuel flow delay time for a reduced power condition. Actually this is a plot of 2.4 inch increase in manifold vacuum or a 50% reduction in power level.

Design Summary

In this chapter, the design of the injector control subcircuits has been described and a statement given to support the selection of each component. In Chapter IX, the test results of this control will be detailed and actual transducer input functions which force the circuit to respond to actual injector and engine characteristics will be presented.

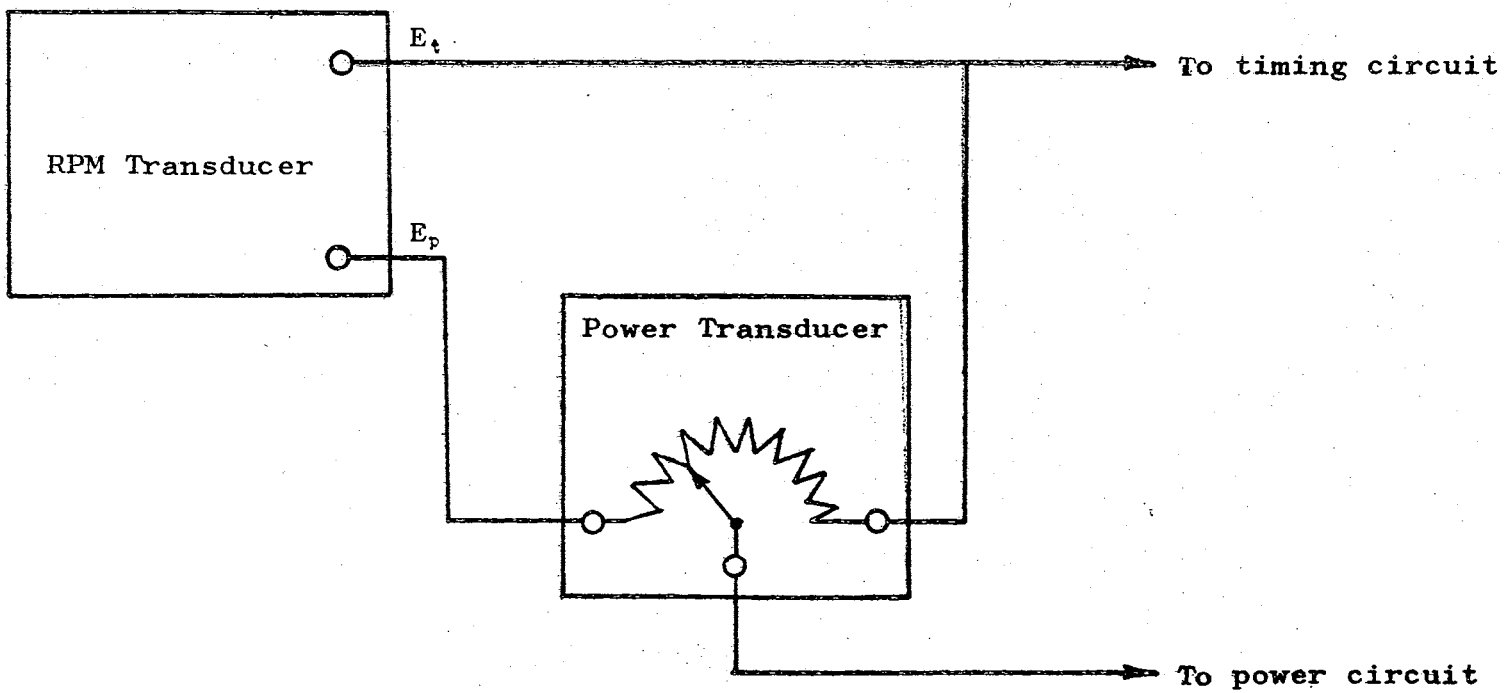

Figure 19. Power Transducer Block Diagram

CHAPTER VIII

DESK TOP ENGINE SIMULATOR

Motor

In order to simplify testing and promote more efficient use of available time for present and future control circuit experimentation, a desk-top engine simulator was designed and built (see Figure 20). The principal component of this simulator is a 12 volt DC variable speed electric motor which simulates the hydrogen engine. A rheostat is used to control motor speed.

Mounted on the front output shaft of the motor is an engine cycle timing switch, a pulley, and a tachometer drive coupling. The rear output shaft drives a two to one reduction gear train that, in turn, actuates three switches.

Speed Pretransducer

The front shaft pulley is used to belt drive a DC generator at an RPM which is a direct function of motor (engine) speed. The voltage output of this generator is linear and is intended as a preliminary signal for the RPM transducer.

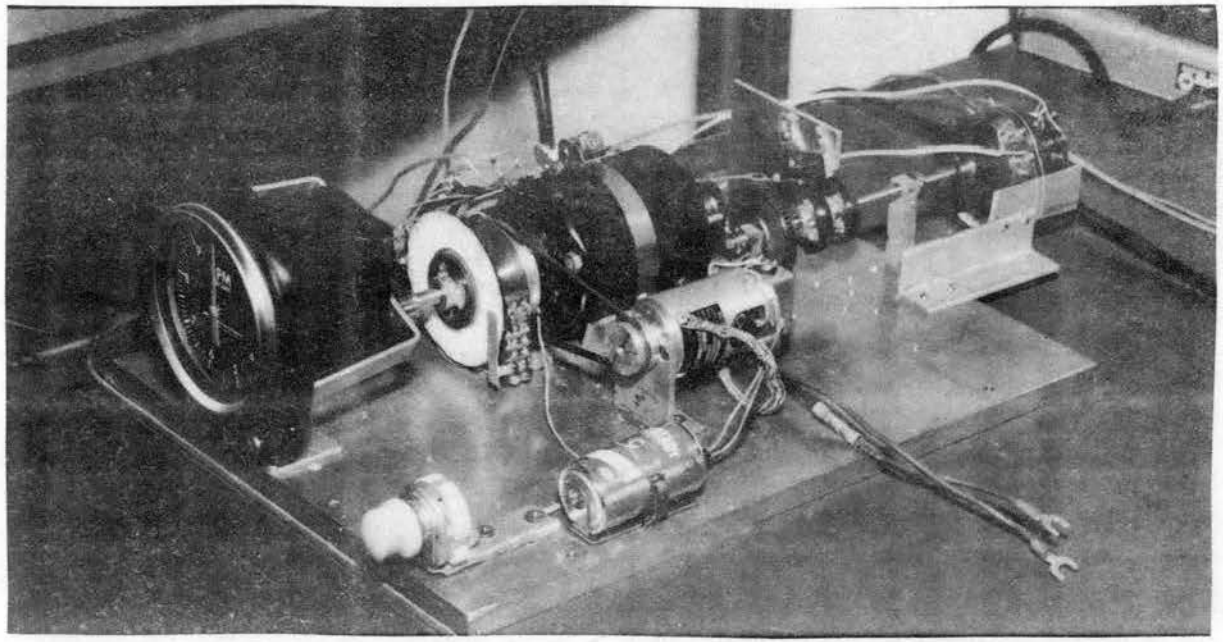

Figure 20. Desk Top Engine Simulator

Engine Cycle Timing Switch

The engine cycle timing switch consists of a circular copper clad phenolic board etched so as to have 10° wide copper segments radiating inward to a copper ring. Between the 10° copper segments is phenolic insulation. A sliding brush is in continuous contact with the inner ring, while a second brush alternately makes contact with a copper segment and breaks contact when it touches a phenolic segment.

Rotation of this disk on the motor output shaft interrupts a DC voltage which is connected in series to an oscilloscope. The pulses displayed on the scope allow the operator to follow the various portions of the engine rotational cycle.

Tachometer

Connected to the front of the motor output shaft is the mechanical tachometer used with the engine test apparatus. The RPM of the simulator can be continuously monitored using this device.

Timing and Reset Switches

Located on the output shaft of the two to one gear reduction drive is one cam actuated microswitch and two precision rotary switches. The rotary switches take the place of the camshaft timing switches while the microswitch simulates the camshaft reset switch of Figure 17.

Operation

The desk-top engine simulator simulates all of the important characteristics of the actual hydrogen engine without encountering the inconvenience associated with actual hydrogen engine operation. With the simulator it has been possible to individually test and trouble shoot each individual subcircuit of the control unit without involving the interaction of other related circuits.

CHAPTER IX

LABORATORY CALIBRATION AND TESTING OF THE CONTROL CIRCUIT

The completed prototype electronic control circuit with the accompanying solenoid actuated injector, with the desk-top engine simulator, and with the test instrumentation used in calibration and testing, is shown in Figure 21.

Instrumentation

Two regulated power supplies were used to simulate the RPM transducer voltage, while two precision digital voltmeters were used to monitor this input.

An oscilloscope was used to monitor injector open and close angles, circuit switching time, and engine rotational position. To accomplish this, the solenoid power voltage and the engine timing signal were superimposed on each other and displayed on the upper scope trace (the first superimposed square wave after the center grid line of Figure 22 is the TDC position of the engine cycle), while the injector valve switch signal was displayed on the lower scope trace. The trigger of the scope was driven by the output of the camshaft timing switch, so that when the switch closed, both the scope trigger and the UJT timing circuits were energized,

[1]Solenoid injector with engine cylinder head.

[2]Switching circuit containing two flip-flop subcircuits.

[3]Injector and fuel flow timing unijunction transistor subcircuit.

[4]Desk top simulator.

- -

Figure 21. Circuit-Simulator Assembly

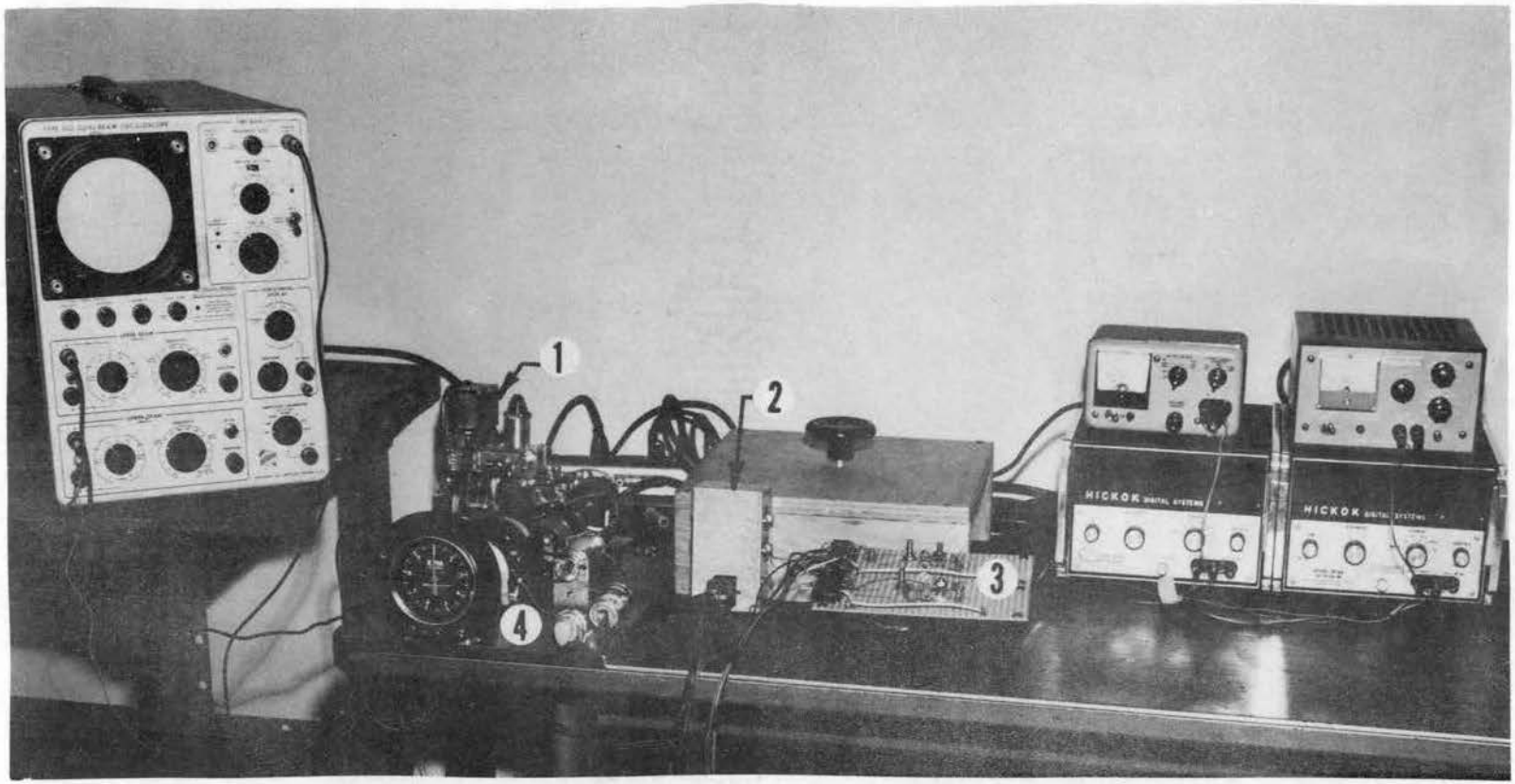

Figure 21. Circuit-Simulator Assembly

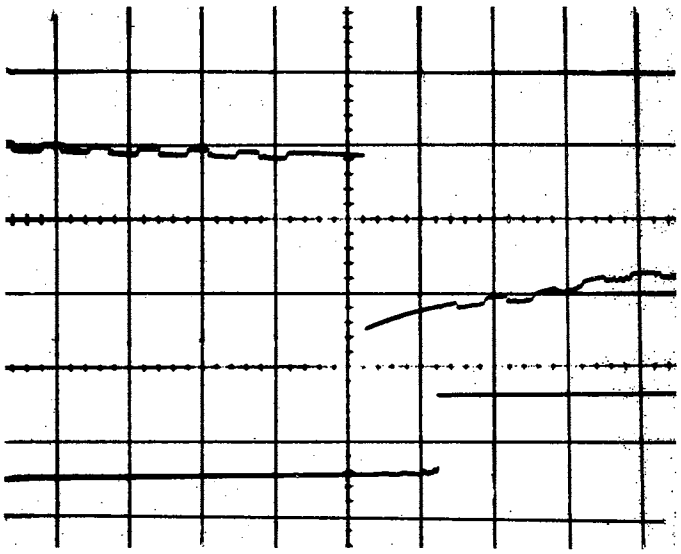

Figure 22. Typical Oscilloscope Display

thereby displaying the time delay between the instant of contact of the camshaft switch and the instant of switching for the respective SCR flip-flop circuit. In addition, the instant of injector valve open and close could be determined relative to engine rotational position by comparing these two signal displays.

Calibration and Testing

Before each test the UJT base voltages, V_{BB}, were set such that each breakover voltage was 4.87 volts. After several preliminary runs, the appropriate values of R_U and R_L (Figure 17) were determined to be 39k ohms while C_U and C_L were determined to be 0.20 and 0.25 microfarads, respectively. The deviations between these actual values and the theoretical values previously mentioned takes into account tolerances in the various electronic components.

Table IV is a tabulation of actual circuit and solenoid valve response after calibration. It is evident from this data that circuit response time is so close to the theoretical values (Figure 13) that the differences between such curves would be indistinguishable if drawn to normal scale. Figure 23 illustrates the variation between theoretical and actual transducer inputs. In each case, a fixed voltage must be added to overcome the voltage drop in the diodes D_U and D_L.

The accuracy of these time and voltage values are limited only by accuracy of scope observations which would

TABLE IV

CONTROL CIRCUIT RESPONSE

RPM	Timing Circuit					Fuel Flow Circuit				
	E_{ct}	E_{ca}	t_t	t_a	φ_o	E_{ct}	E_{ca}	t_t	t_a	φ_c
1000	5.02	5.40	26.3	26.5	+15	5.02	5.37	26.3	25.5	+17
1500	5.70	6.08	14.5	14.0	+ 5	5.44	5.79	16.9	16.5	-12
2000	6.58	6.96	10.1	10.0	+ 2	5.94	6.29	12.9	13.0	-25
2500	7.61	7.99	7.66	7.7	0	6.54	6.89	10.2	10.2	-38
3000	9.28	9.66	5.58	5.5	- 2	7.27	7.62	8.3	8.5	-48
3500	11.88	12.26	3.96	4.0	- 5	8.18	8.53	6.8	7.0	-55
4000	16.51	16.89	2.62	2.6	---	9.37	9.83	5.5	5.8	-60

Note: E_{ct} = Theoretical emitter breakover voltage.

E_{ca} = Actual emitter breakover voltage.

t_t = Theoretical circuit response time.

t_a = Actual circuit response time.

φ_o = Injector valve open angle.

φ_c = Injector valve close angle.

Positive angles indicate degrees before top dead center.

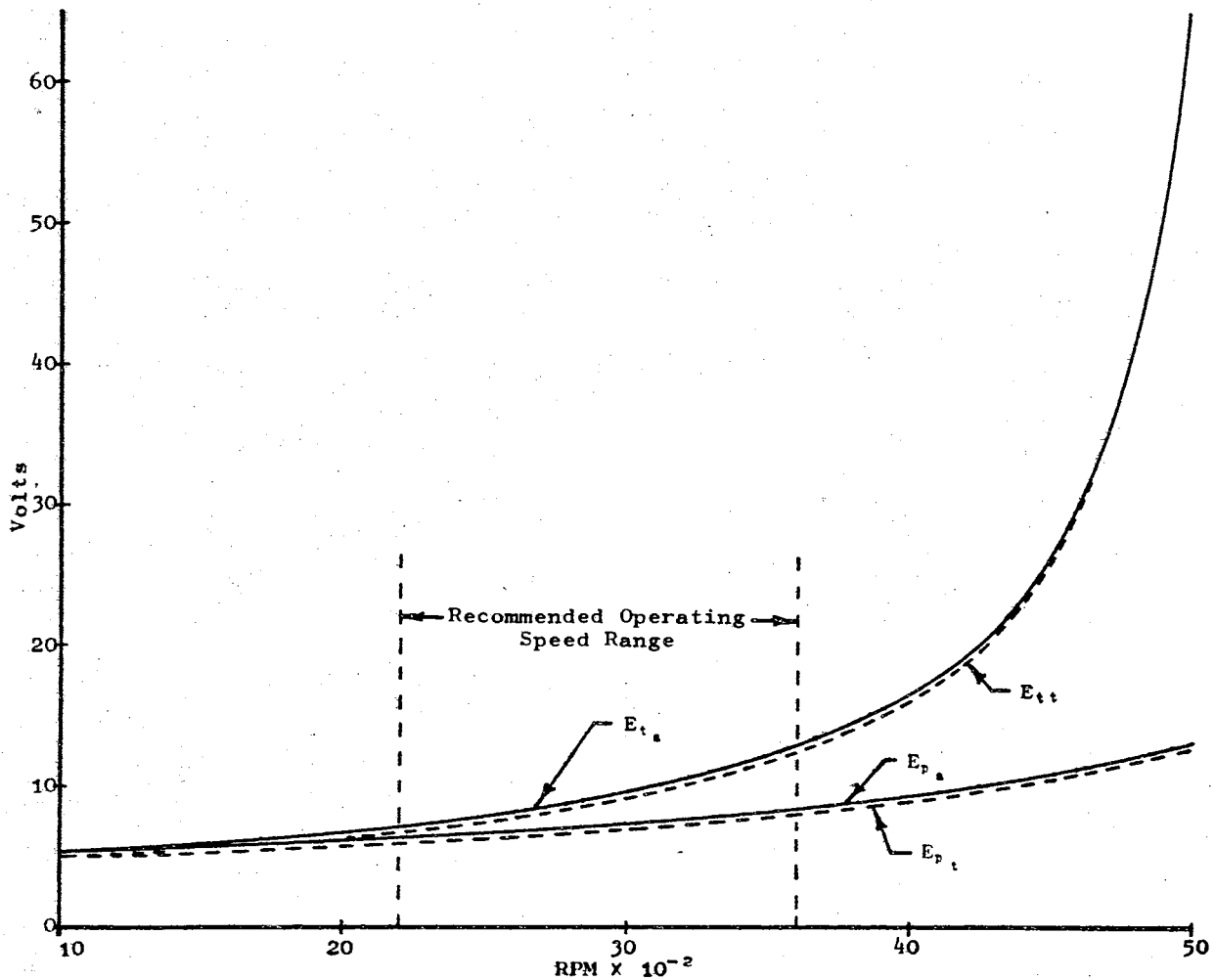

Figure 23. Actual Transducer Inputs

range from a condition of one millisecond error while observing a 25 millisecond signal on the five millisecond per centimeter scope scale or

$$\frac{1}{25} (100) = 4\%$$

to a 0.1 millisecond error while observing a two millisecond signal on the one millisecond per centimeter scope scale or

$$\frac{0.1}{2} (100) = 5\%.$$

Both of these inaccuracies are considered quite acceptable for this type of analysis.

The determination of injection time relative to engine angular position was the least accurate of all measurements. This was caused by the inaccuracy in the tachometer and the difficulty in maintaining an exact engine simulator RPM. The tachometer has an accuracy of ±1% of 10,000 RPM or ±100 RPM. In the design operating range of this engine (0-5000 RPM), this represents 2% of maximum speed. The difficulty of reading this meter to ±100 RPM combined with the difficulty of maintaining a constant simulator speed yielded maximum angular deviations of up to 10° from the expected value.

The above angular errors are not considered serious in this engine since experiments with the mechanical injector engine show satisfactory engine performance results over wide ranges of injection initiation angles.

Particular Design Outline

When an improved solenoid injector valve is developed, it should be a relatively simple task to adapt this valve and the previously described control circuit to any conventional engine. A description of the basic adaptation procedure follows:

1) Determine the solenoid pick-up time and solve Equation (2) over the desired operating range.
2) Determine the camshaft timing switch preset.
3) Match the curve generated by this particular solution of Equation (2) to an acceptable range of Equation (4), using as a guideline, values of $\frac{E_c}{E}$ less than about 0.98. This specifies the relationship between E and RPM.
4) Assign R_U a value such that the product of $R_U C_U$ yields the value shown in Equation (4) of step 3. Note that values of C_U lower than 0.2 microfarads are generally undesirable.
5) Assign a maximum value of R_L in the power transducer such that the $R_L C_L$ product agrees with Equation (4) step 3. Note that values of C_L less than 0.2 microfarads are also undesirable.
6) Calibrate the circuit and adjust resistances R_U and R_L to compensate for component tolerances.
7) Match input voltage values, E, of step 3 to

RPM transducer outputs, and match the resistance output of the power transducer to the circuit requirements.

8) Assemble circuit and peripheral equipment and make final tests on the engine simulator.

9) Assemble completed system on the engine and make final adjustment.

CHAPTER X

SUMMARY AND CONCLUSIONS

Scope of the Problem

The scope of the problem detailed in this dissertation can be subdivided into the following phases:

1) Perform a preliminary design study.
2) Design and fabricate a prototype mechanical injector research engine.
3) Design and fabricate an engine test facility.
4) Determine, by testing, this engine's characteristics when fueled with iso-octane.
5) Test, modify, and retest this engine when fueled with hydrogen.
6) Design, fabricate, and test a prototype control circuit for use on a hydrogen fueled engine.

Conclusions

Preliminary Design Analysis

Preliminary research indicated that successful hydrogen engine development might be possible if two problems could be overcome. The first of these was engine knock caused by

detonation and preignition. The second was excessive engine operating temperatures as experienced when pure oxygen was used as the oxidizer.

Mechanical Injector Design and Fabrication

With the above two problems in mind, the mechanical injector engine was designed with the basic approach of modifying a conventional single cylinder industrial engine to incorporate a camshaft operated injector for hydrogen fuel delivery. This modification included:

1) Design of an injector and injector drive mechanism.
2) Design of a variable timing ignition system.
3) Design of a strobe-light timing system incorporating a vibration dampening flywheel.
4) Conversion and installation of an electric starting system.
5) Modification of the air-induction system to incorporate a float type carburetor.
6) Modification of the basic engine to accept the above systems and associated instrumentation.

Engine Test Facility

A water-brake type dynamometer was chosen as the central device in the test apparatus. Around this dynamometer, both an iso-octane and a hydrogen fuel supply system were

added. Provision was made to monitor crankcase, cylinder head, and exhaust gas temperatures as well as engine operation time. Air and fuel flow meters were installed to complete the instrumentation.

Iso-Octane Engine Tests

One hundred twenty-three test runs were made with the iso-octane fueled counterpart of the hydrogen engine. Complete engine operational characteristics as well as operator training and facility testing were determined during these runs. The data collected led to the establishment of the basic fuel requirement theories needed to formulate a design of the electric injection control system.

Hydrogen Engine Operation

Utilizing the basic mechanical injector design described above, the hydrogen engine was operated for over $4\frac{1}{2}$ hours on both glow and spark plug ignition. Spark plug ignition was found to be preferable.

Preliminary emphasis was placed on a continuous modification program rather than on performance testing. This direction led to establishment of knock-free performance under all operating speeds and up to about 50% power. Solutions to both of the above mentioned research problems, knock and excessive temperatures, were achieved under experimental conditions.

Control Circuit Design, Fabrication and Test

By incorporating two SCR flip-flop switching circuits with two RC time delay circuits and a reset circuit, a prototype electric injection control device was developed that accurately timed a pair of solenoid injectors. Both the injection initiation and termination times were controlled within acceptable tolerances.

Discussion

The high energy content and clean reaction products of hydrogen make it a desirable motor fuel. The difficulties of engine knock, handling safety, and cost have, however, tended to prevent its use as a practical fuel in the past.

The disadvantage of incorporating an injection system in an engine design is partially offset by the following advantages: first, the need for cold starting mixture enrichment is eliminated since hydrogen has no difficulty vaporizing in any normal temperature region. Second, an acceleration enrichment device is not needed since hydrogen will always remain in the gaseous state. Also, its wide flammability limits allow larger tolerances in air-fuel ratio control.

Recent efforts in space and missile research have decreased the cost of liquid hydrogen to about fifty cents per

pound and have greatly increased the safety of its handling (14).

Since research leading to this dissertation has shown that it may be possible to build a knock-free engine, it is conceivable that a practical engine may be developed that can replace the present fossil fueled engine and thereby help combat air pollution.

Suggested Future Research

The preliminary work recorded herein has only shown one direction that could be taken in the development of a practical hydrogen engine. Considering the urgency in the development of a nonpolluting mobile power plant for today's civilization, it would seem desirable to stimulate further research in the following areas:

1) Development of a practical mechanical injector engine.
2) Further improvement and miniaturization of the electric injector control.
3) Development of peripheral devices to be used with the control circuit.
4) Completely optimize a hydrogen fueled reciprocating engine.

Actually, each of the foregoing items could easily be broken down into numerous sub-areas for individual research and planning.

BIBLIOGRAPHY

(1) Cole, Lamont C. "Can the World be Saved," paper presented at 134th annual meeting of American Association for the Advancement of Science, January, 1968.

(2) Erren and Campbell. "Hydrogen: A Commercial Fuel for Internal Combustion Engines and Other Purposes." Journal of the Institute of Fuel, Vol. VI (June, 1933), pp. 277-290.

(3) Heinze, Edwin P. A. "Hydrogen Engines for Off-Peak Power Utilization." Power (February, 1933), pp. 90-92.

(4) King, R. O. et al. "The Hydrogen Engine and the Nuclear Theory of Ignition." Canadian Journal of Research, Vol. 26, Section F (June, 1948), pp. 264-276.

(5) Morgan, N. E., and W. D. Morath. Development of a Hydrogen-Oxygen Internal Combustion Engine Space Power System, NASA CR-255, Detroit, Michigan: Vickers, Inc., July, 1965.

(6) Haines, C. A., and T. E. Redding. The Hypergolic Reciprocating Engine Electrical Power System and Its Application to the Lunar Excursion Module, NASA working paper No. 1202, Houston, Texas: NASA, April, 1966.

(7) North American Combustion Handbook, The North American Manufacturing Co., 1952.

(8) Provisional Workshop Manual. Fuel System, Volkswagon Corporation, Wolfsburg, Germany, 1968.

(9) Crouse, William H. Automotive Mechanics. 5th ed. New York: McGraw-Hill, 1956.

(10) Lytel, Allan. Silicon Controlled Rectifiers. New York: Howard W. Sams and Co., Inc., 1967.

(11) Silicon Controlled Rectifier Manual. 2nd ed. New York: General Electric Company, 1961.

(12) Heller, Saul. Understanding Silicon Controlled Rectifiers. New York: Hayden Book Co., 1968.

(13) Transistor Manual. New York: General Electric Company, 1964.

(14) Lessing, Lawrence. "The Master Fuel of a New Age." Fortune (May, 1961), pp. 152-244.

(15) Schoeppel, R. J., and R. G. Murray. "The Development of Hydrogen Burning Engines." (Paper presented at Frontiers of Power Technology Conference, Oklahoma State University, 1968), p. 12.

(16) Murray, R. G., and R. J. Schoeppel. "A Progress Report on the Development of OSU's Hydrogen-Burning Engine." (Paper presented at Frontiers of Power Technology Conference, Oklahoma State University, 1969), p. 14.

APPENDIX A

ENGINE TEST AND PERFORMANCE DATA

One hundred twenty-three experimental test runs were performed on the B & S test engine using ASTM iso-octane fuel. The first 19 tests were made with various mixture and power settings required for training personnel. Runs 20-123 were at maximum attainable power under various speeds and ignition timings.

A condition believed to be a harmonic resonance at 3000 RPM yielded consistent low horsepower and torque readings during these runs. Also, vibration and erratic float operation caused large fluctuation in the recorded fuel flow in some cases.

A refined test procedure was incorporated for fuel flow measurement and the 3000 RPM speed was avoided in runs 80-123. Between run numbers 96 and 123, the throttle was progressively closed from 100% to 80%, 60%, 40%, 20%, and 15% of linear motion of the throttle lever on the dynamometer. All runs after number 96 were at 15° before top dead center.

Various plots of the data were made. Three important plots, however, are presented as Figures 5, 6, and 7 of this report. Figure 24 and the succeeding page is a flow diagram

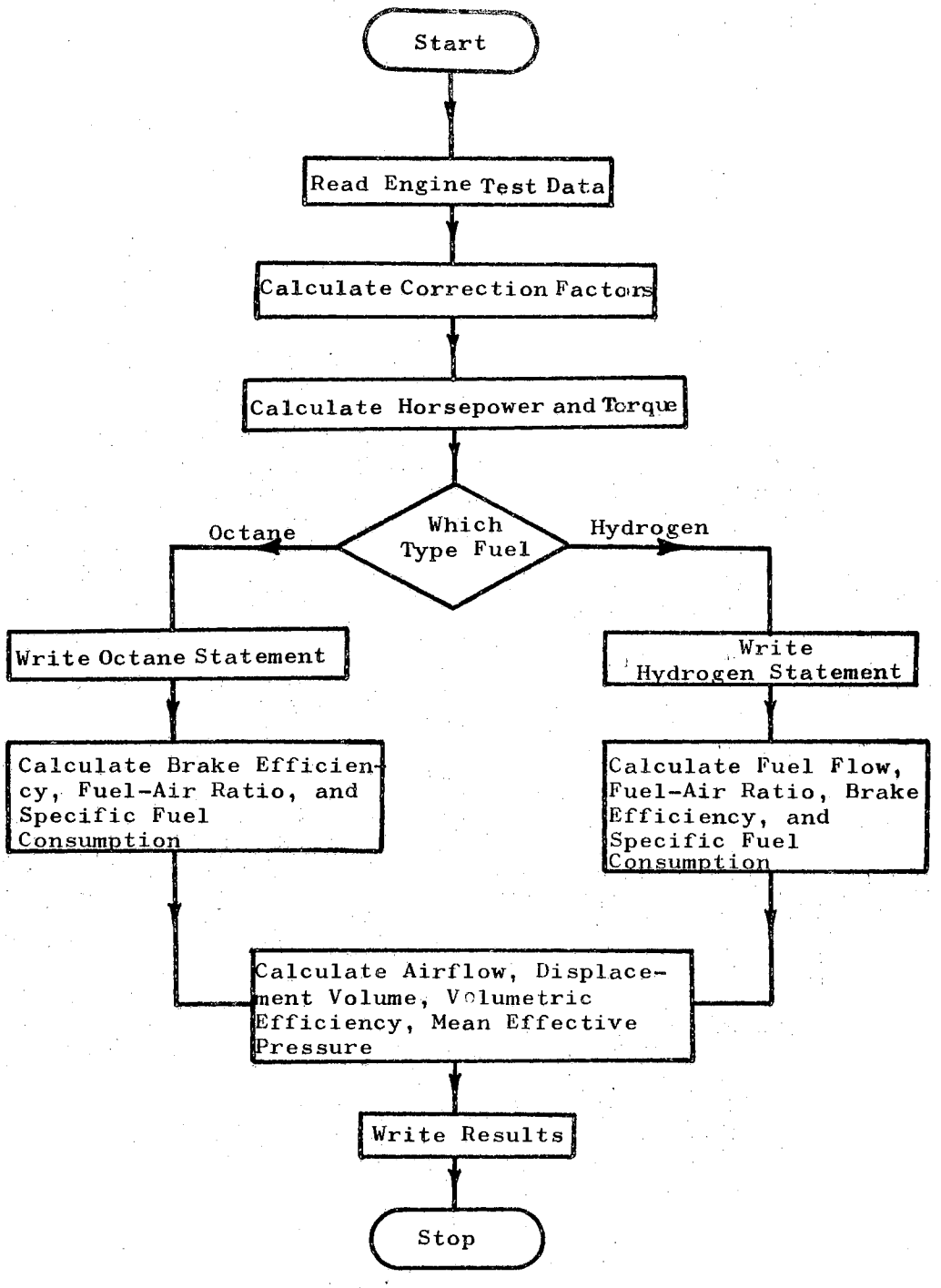

Figure 24. Engine Computer Program Flow Diagram

```
00000000011111111112222222222333333333344444444445555555555666666666677777777778
12345678901234567890123456789012345678901234567890123456789012345678901234567890
      1 READ(5,2)I
      2 FORMAT(I3)
        J=0
        REAL MFPRES
        INTEGER ARTEMP,RPM,EXTEMP,CHTEMP,CRTEMP,P1,P2,T1,T2
      3 READ(5,4)ARTEMP,BPRES,HUMCF,RPM,POUND,AIRFLO,GASFLO,EXTEMP,CHTEMP,
     CCRTEMP,MFPRES,IGN,P1,P2,T1,T2,TIM,ZFACT1,ZFACT2,INJECP
      4 FORMAT(I2,F4.2,F5.4,I4,2F3.1,F3.2,2I4,I3,F4.2,5I4,F4.2,2F4.3,I4)
C       BORE,STROKE,PISTON DISPLACEMENT, AND CLEARANCE VOLUME ARE IN INCHES
        BORE=2.500
        STROKE=2.125
        PD=10.72
        CLVOL=2.08
        CR=6.18
      6 FORMAT(2X,2HHP,3X,1HT,3X,3HF/A,3X,4HEFBT,1X,4HBSFC,1X,4HEFVL,1X,4H
     CBMEP,2X,3HPCF,3X,3HTCF,3X,3HHCF,3X,5HFORCE,1X,4HAFLO,2X,4HFFLO,1X,
     C2HAT,1X,4HEX-T,2X,3HCHT,1X,3HCRT,1X,5HBARPR,1X,5HMANPR,2X,3HIGN,2X
     C,5HACT-V,2X,5HTHE-V,3X,3HRPM,/)
C       PERFORM CALCULATIONS-TORQUE IS IN FOOT POUNDS
C       CORRECT TO STANDARD CONDITIONS
        PRESCF=1.000-0.0396*(BPRES-29.95)
        TEMPCF=1.000+0.000915*(ARTEMP-60)
        ARFLOW=AIRFLO*PRESCF*TEMPCF*HUMCF
     12 HP=(POUND*RPM/10000)*PRESCF*TEMPCF*HUMCF
     13 TORQUE=(HP*10000*0.525)/RPM
      7 IF(GASFLO)45,16,9
      9 WRITE(6,10)
     10 FORMAT(1X,44HTHIS IS AN OCTANE BURNING ENGINE CALCULATION,///)
        FULAIR=GASFLO/ARFLOW
     14 EFFBTH=HP*2545/(GASFLO*19000)
C       BSFC IS IN POUNDS PER BHP HOUR
     15 BSFC=GASFLO/HP
        GO TO 20
     16 WRITE(6,17)
     17 FORMAT(1X,45HTHIS IS A HYDROGEN BURNING ENGINE CALCULATION,///)
        VOL=3.14
        HYDFLO=(VOL*60/(TIM*767))*(((P1+(BPRES*0.491))/((T1+460)*ZFACT1))-
       C((P2+(BPRES*0.491))/((T2+460)*ZFACT2)))*144
        GASFLO=HYDFLO
        FULAIR=HYDFLO/ARFLOW
        EFFBTH=HP*2545/(HYDFLO*46850)
        BSFC=HYDFLO/HP
        GO TO 20
C       AIRFLOW IS IN POUNDS PER HOUR
     20 ACTVOL=(ARFLOW*53.35*(ARTEMP+460))/(144*0.491*BPRES)
        THEVOL=60*RPM*(PD/(2*1728))
     21 EFFVOL=ACTVOL/THEVOL
     22 BMEP=HP*2545*778/(THEVOL*144)
        WRITE(6,6)
        WRITE(6,25)HP,TORQUE,FULAIR,EFFBTH,BSFC,EFFVOL,BMEP,PRESCF,TEMPCF,
       CHUMCF,POUND,AIRFLO,GASFLO,ARTEMP,EXTEMP,CHTEMP,CRTEMP,BPRES,MFPRES
       C,IGN,ACTVOL,THEVOL,RPM
        J=J+1
        IF(J-I)3,50,50
     25 FORMAT(1X,F4.2,1X,F4.2,1X,F5.3,1X,F6.2,1X,F4.2,1X,F4.2,1X,F4.0,1X,
       CF5.3,1X,F5.3,1X,F6.4,1X,F4.1,1X,F5.1,1X,F5.2,1X,I2,1X,I4,1X,I4,1X,
       CI3,1X,F5.2,1X,F5.2,1X,I4,1X,F6.1,1X,F6.1,2X,I4,///)
     45 WRITE(6,46)
     46 FORMAT(1X,25HGASFLOW VALUE IS NEGATIVE)
        GO TO 50
     50 STOP
        END
```

and computer program which was used to calculate the final data used in constructing these graphs.

APPENDIX B

COMPUTER PROGRAM FOR INJECTOR SYNCHRONIZATION

The following program solves Equation (4) of Chapter VI for various values of

$$0.0500 \leq \frac{E_o}{E} \leq 0.9999$$

and

$$0.001 \leq RC \leq 0.010.$$

A plot of the family of curves thus generated allows the selection of the curve that most closely approximates the curve of Equation (2) of Chapter VI. This procedure, therefore, defines the electric circuit which simulates the mechanical behavior of an engine.

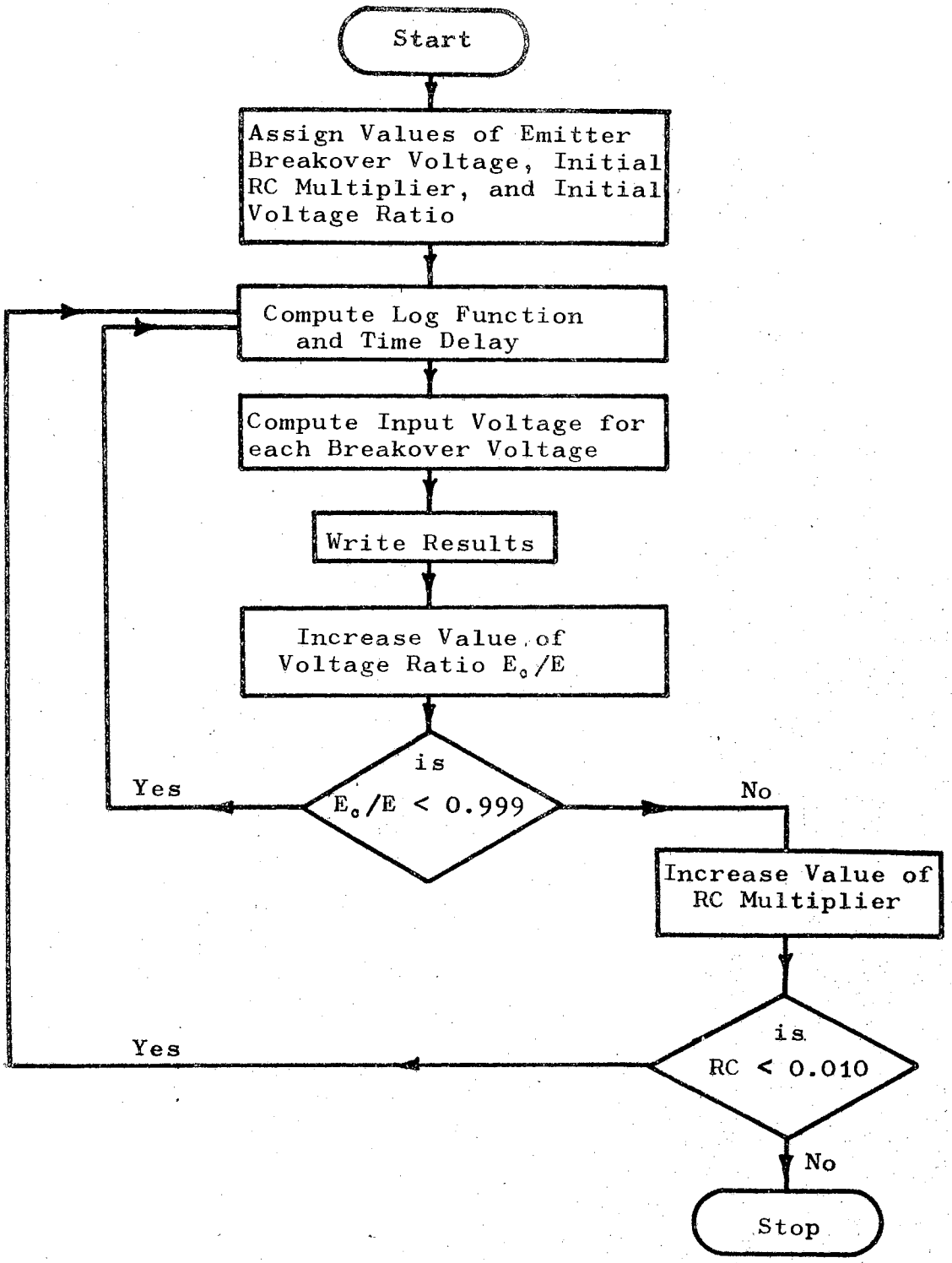

Figure 25. Flow Diagram for Injector Synchronization Program

```
00000000011111111112222222222333333333344444444445555555555666666666677777777778
12345678901234567890123456789012345678901234567890123456789012345678901234567890

      REAL LN
      RC=0.001
      EC1=4.87
      EC2=4.87
    2 EOE=0.0500000
    3 LN=ALOG(1/(1-EOE))
      T=RC*LN
      EIN1=EC1/EOE
      EIN2=EC2/EOE
      WRITE(6,4)T,RC,LN,EOE,EIN1,EIN2
    4 FORMAT(1X,2HT=,F8.6,1X,3HSEC,5X,3HRC=,F7.5,5X,3HLN=,F7.5,5X,4HEOE=
     C,F6.4,5X,5HEIN1=,F6.2,1X,5HVOLTS,5X,5HEIN2=,F6.2,1X,5HVOLTS)
      EOE=EOE+0.1
      IF(EOE-0.9999)3,5,5
    5 RC=RC+0.0005
      IF(RC-0.010)2,6,6
    6 STOP
      END
```

VITA

3

Richard George Murray

Candidate for the Degree of

Doctor of Philosophy

Thesis: A HYDROGEN ENGINE AND CONTROL CIRCUIT DESIGN

Major Field: Engineering (Mechanical)

Biographical:

Personal Data: Born in Omaha, Nebraska, January 24, 1934, the son of Mr. and Mrs. George Roy Murray; married Nancy Rhoads, 1957; two sons: Justin, age 8, and George, age 6.

Education: Graduated from Hastings High School, Hastings, Nebraska, June, 1951; attended Hastings College, Hastings, Nebraska, 1951 to 1953; received the Bachelor of Science degree in Mechanical Engineering from Southern Methodist University in 1959; received the Master of Science degree in Mechanical Engineering from Missouri School of Mines in 1962; completed requirements for the Doctor of Philosophy degree at Oklahoma State University in May, 1970.

Professional Experience: Co-op Engineer, Convair Aircraft Corporation/Fort Worth, 1956-59; Assistant Professor, Missouri School of Mines, 1959-64; Assistant Professor, Western Michigan University, 1964-68; Mechanical Engineering Education Advisor to Technical College, Ibadan, Nigeria on the Western Michigan University-USAID Project, 1965-68; Graduate Research Assistant, Oklahoma State University, 1968-70.